

# Electromagnetic structure of the nucleon and the Roper resonance in a light-front quark approach

Igor T. Obukhovskiy,<sup>1</sup> Amand Faessler,<sup>2</sup> Thomas Gutsche,<sup>2</sup> and Valery E. Lyubovitskij<sup>2,3</sup>

<sup>1</sup>*Institute of Nuclear Physics, Moscow State University, 119991 Moscow, Russia*

<sup>2</sup>*Institut für Theoretische Physik, Universität Tübingen,  
Kepler Center for Astro and Particle Physics,*

*Auf der Morgenstelle 14, D-72076, Tübingen, Germany*

<sup>3</sup>*Department of Physics, Tomsk State University, 634050 Tomsk, Russia*

(Dated: March 12, 2018)

A relativistic light-front quark model is used to describe both the elastic nucleon and nucleon-Roper transition form factors in a large  $Q^2$  range, up to 35 GeV<sup>2</sup> for the elastic and up to 12 GeV<sup>2</sup> for the resonance case. Relativistic three-quark configurations satisfying the Pauli exclusion principle on the light-front are used for the derivation of the current matrix elements. The Roper resonance is considered as a mixed state of a three-quark core configuration and a molecular  $N + \sigma$  hadron component. Based on this ansatz we obtain a realistic description of both processes, elastic and inelastic, and show that existing experimental data are indicative of a composite structure of the Roper resonance.

PACS numbers: 12.39.Ki, 13.40.Gp, 13.40.Hq, 14.20.Gk

Keywords: Roper resonance, quark model, hadron molecules, strong and electromagnetic form factors

## I. INTRODUCTION.

The last decade has been marked by significant progress in the experimental study of low-lying baryonic resonances (the radial/orbital nucleon excitations with  $J^P = \frac{1}{2}^\pm, \frac{3}{2}^\pm$ ). Specifically new insights have been obtained in  $\pi$  [1] and  $2\pi$  [2] electroproduction on the proton with the polarized electron beam at JLab (CLAS Collaboration) followed by a combined analysis of pion- and photoinduced reactions made by CB-ELSA and the A2-TAPS collaborations [3]. Electro- and photoproduction of these resonances is recognized as an important tool which allows to study the relevant degrees of freedom, wave functions and interactions between constituents and the transition to perturbative quantum chromodynamics (pQCD).

The structure issue of the lowest-lying nucleon resonance  $N(1440)$  with  $J^P = \frac{1}{2}^+$  (the Roper resonance  $P_{11}$  or simply  $R$ ) is a longstanding problem of hadron physics. One indication that the inner structure of the Roper is possibly more complicated than the structure of the other lightest baryons was first obtained in the framework of the constituent quark model (CQM). It was found that the observed mass of the Roper resonance is much too low and the decay width is too large when compared to the predicted values of the CQM. The simplest description of the Roper consists of the three-quark ( $3q$ ) configuration  $sp^2[3]_X$ , i.e. the first ( $2S$ ) radial excitation of the nucleon ground state  $s^3[3]_X$ , but it fails to explain either the large decay width  $\Gamma_R \simeq 300$  MeV or the branching ratios for the  $\pi N$  (55%–75%) and  $\sigma N$  (5%–20%) decay channels [3, 4].

Evaluation of these values in the framework of the CQM is often based on the elementary emission model with single-particle quark-meson (or quark-gamma) cou-

plings  $qq\pi$ ,  $qq\sigma$ ,  $qq\gamma$ , etc. The calculation of decay widths (or of the electroproduction cross section at small virtuality of the photon with  $Q^2 \simeq 0$ ) results in anomalous small values. These underestimates for the decay matrix elements can especially be traced to the strict requirement of orthogonality for the ground ( $0S$ ) and excited state ( $2S$ ) radial wave functions of the  $N$ - and  $R$  states belonging to quark configurations with the same spin-isospin ( $S = 1/2$ ,  $T = 1/2$ ) and symmetry ( $[3]_{ST}[3]_X$ ) quantum numbers. To overcome this discrepancy it is suggested that either the Roper is not an ordinary  $3q$  state or the "true" transition operators have a more complicated form than the single-particle operators used in the CQM calculations.

The elementary theory of strong interactions QCD provides a framework, which is directly usable only at high momentum transfers. Nevertheless, the discussed data [1–3] span the range from soft to hard momentum transfers  $0 \leq Q^2 \lesssim 4 - 5$  GeV<sup>2</sup> (up to  $\sim 12$  GeV<sup>2</sup> for the JLab upgrade). A major challenge for theory is that a quantitative description of the transition amplitudes must also include soft nonperturbative contributions. For the soft region there are important results from lattice QCD with "unquenched"  $\bar{q}q$  degrees of freedom [5, 6] but the present computer capabilities do not allow us yet to extract all the hadron properties in a systematic way.

Other approaches that are directly connected to QCD are either based on light cone sum rules [7] (in reality they can be used at  $Q^2 \gtrsim m_{N^*}^2$ ) or on Dyson-Schwinger equations (DSEs) [8–10]. A DSE study [10] produces a radial excitation of the nucleon in the quark-diquark basis at  $\sim 1.82$  GeV. Pion electroproduction amplitudes in the resonance region  $W \simeq m_R$  are successfully analyzed in terms of the dynamical coupled channel model [11–13], which is used at the Excited Baryon Analysis Center at JLab. Combining both methods, Refs. [9, 11] demon-

strate that the Roper resonance is indeed the first radial excitation of the proton, but the Roper “obscures its dressed-quark core with a dense cloud of pions and other mesons” [9].

The  $\sigma$  meson along with the uncorrelated pion cloud possibly play a key role in the inner structure of the Roper. This mechanism was proposed in Ref. [14] where the authors showed that in  $\pi N$  scattering the intermediate  $\sigma N$  state defines the Roper resonance pole. Thus there is no need for some special quark configuration of the type  $sp^2[3]_X$  to describe the Roper resonance contribution to the physical processes.

It is clear that the nature of the low-lying baryonic resonances is still an unresolved issue and in this respect the study of the  $Q^2$ -behavior of their electroproduction amplitude is of much current interest. Since direct QCD calculations are difficult in the low-energy regime several models for the electroexcitation of the Roper resonance were proposed during the last three decades [15–22] (see reviews [23, 24] for details). Now model predictions can be compared to the new high-quality photo- and electroproduction data [1–3]. Updated versions [25–28] of the most realistic models were used to give a good description of the data at intermediate values of  $1.5 \lesssim Q^2 \lesssim 4 \text{ GeV}^2$ . However, in the soft region, i.e. at low values of  $Q^2$  ( $0 \leq Q^2 \lesssim 1 - 1.5 \text{ GeV}^2$ ), the data qualitatively differ from theoretical predictions made in the framework of quark models without meson cloud.

Recently the electromagnetic nucleon-Roper transition has been studied in the framework of anti-de Sitter AdS/QCD [29, 30]. In particular, in Ref. [29] the Dirac form factor for the electromagnetic nucleon-Roper transition has been calculated in light-front holographic QCD. In Ref. [30] the Roper electroproduction was considered in a soft-wall AdS/QCD model [31–33] with inclusion of the leading three-quark ( $3q$ ) state and higher Fock components.

As a result there are essentially three comprehensive theoretical approaches to the Roper electroproduction on the market. One of them (the coupled channel model of the meson cloud [2, 12, 13, 34]) is successful in the soft region  $0 \leq Q^2 \lesssim 1 \text{ GeV}^2$  and, the other one, the LF three-quark model [19, 20, 25, 28] or the covariant quark spectator model [26]) is compatible with data in the hard region  $Q^2 \gtrsim m_N^2 - 2m_N^2$ . The third approach is based on a novel method to hadronic structure — AdS/QCD [29, 30].

In our recent work [35] we obtained a quantitative description of the Roper electroproduction helicity amplitudes in the region  $0 \leq Q^2 \lesssim 2 \text{ GeV}^2$  where we started with the following model principles:

- (i) “Unquenching” of the constituent quark model, i.e. taking into account the  $q\bar{q}$  pair effects (e.g., see the discussion in Ref. [36]) in the soft- $Q^2$  region. This leads to a nonlocal  $qq\gamma$  coupling depending on the inner momentum of the  $q\bar{q}$  wave function of the intermediate vector meson [the vector meson dominance (VMD) is implied].
- (ii) Smooth transition from the “soft” nonlocal electro-

magnetic coupling to the “hard” one with growing momentum transfer  $Q^2$ . In the hard region the nonlocal  $qq\gamma$  coupling reduces to the standard  $Q^2$ -dependent quark form factor characteristic of the VMD model.

- (iii) The hadron-molecular  $N + \sigma$  state is considered as a possible component of the Roper wave function along with the radial excitation of the three-quark configuration.

Although nonrelativistic quark configurations were used, a realistic description of the  $Q^2$  dependence of transition amplitudes was obtained in a large interval of momentum transfers  $0 \leq Q^2 \lesssim 1.5 - 2 \text{ GeV}^2$ . Given the quality of the suggested model it reinforces the statement that symmetry principles (e.g. the Pauli principle for quark systems including the  $3q + q\bar{q}$  component, the VMD in the electromagnetic coupling, etc.) play the decisive role in the description of the electroexcitation of low-lying resonances.

Starting from the results of Ref. [35] we developed a relativistic version of the suggested electroexcitation mechanism. Wave functions of baryons are set up in a LF constituent quark model based on the relativistic Hamiltonian dynamics which was first formulated by Berestetskii and Terent’ev [37] and applied to various hadronic processes in Refs. [18, 19, 25, 28, 38–42].

The paper is structured as follows. First, in Sec. II, we briefly discuss the LF formalism relevant for the electroproduction processes. In Sec. III we fit the parameters of the model to the elastic  $e - N$  data (up to  $Q^2 \approx 35 \text{ GeV}^2$ ) including the limit  $Q^2 \rightarrow 0$  (magnetic moments). The quality of fit in describing the nucleon form factors is a test of our version of the LF approach to the nucleon electromagnetic coupling. We further use this model in Sec. III for the description of the quark core contribution to the electroproduction amplitudes. In the framework of our model for the Roper resonance considered as a composite state [35] we calculate the helicity amplitudes  $A_{1/2}$  (transverse) and  $S_{1/2}$  (longitudinal) for the Roper resonance electroproduction on the nucleon. The results obtained are compared to the recent CLAS data (up to  $Q^2 \approx 4 - 5 \text{ GeV}^2$ ). Predictions for higher values of  $Q^2$  (up to  $12 \text{ GeV}^2$  for the JLab upgrade) are also discussed. Finally, in Sec. IV, we summarize our results.

## II. DEFINITION OF FORM FACTORS IN TERMS OF THREE-QUARK CONFIGURATIONS ON THE LIGHT-FRONT

The light-front approach [37–40] to elastic and inelastic nucleon form factors was used in many works in the last three decades [18–20, 24, 25, 28, 36, 40–42]. We follow Refs. [18, 19, 40–42] where the method was described in many details. Here we only accentuate some aspects which are not covered in the literature but which are essential for us in the study of the nucleon form factors. In addition in Sect. II C we cite several well known formulas from Ref. [40] to allow an easier reading of our

manuscript.

### A. Melosh rotation in the $3q$ system

First of all it should be noted that the Melosh rotation

$$R_M^{(i)}(x_i, \mathbf{k}_{\perp i}, \mathcal{M}_0) = \frac{m_i + x_i \mathcal{M}_0 - i \boldsymbol{\sigma} \cdot [\hat{\mathbf{z}} \times \mathbf{k}_{\perp i}]}{\sqrt{(m_i + x_i \mathcal{M}_0)^2 + \mathbf{k}_{\perp i}^2}} \quad (1)$$

(we use standard kinematical parameters  $m_i, x_i$  and  $\mathbf{k}_{\perp i}$  of the  $i$ th quark, which are defined below) is not a trivial operation in the case of a three-fermion system which should satisfy the Pauli exclusion principle. Sometimes the product of three independent rotations

$$\mathcal{R}_M = \prod_{i=1}^3 R_M^{(i)} \quad (2)$$

produces a change in the type of initial permutational symmetry (the Young scheme) of the  $3q$  wave function.

If one suggests that the wave function is defined by a certain LF dynamics such a function should satisfy the Pauli exclusion principle. In reality we start from the canonical ( $c$ ) quark spin wave function defined in the rest frame, where the fully symmetric spin-isospin ( $ST$ ) state of three quarks (the Young scheme  $[3]_{ST}$ ) has the following (allowed by the Pauli principle) form:

$$|[3]_{ST}, \mu', t\rangle_c = \sqrt{\frac{1}{2}} |[21]_S y_S^{(1)}, \mu'\rangle_c |[21]_T y_T^{(1)}, t\rangle + \sqrt{\frac{1}{2}} |[21]_S y_S^{(2)}, \mu'\rangle_c |[21]_T y_T^{(2)}, t\rangle \quad (3)$$

[for  $S=1/2$  (or  $[21]_S$ ) and  $T=1/2$  (or  $[21]_T$ )]. Here we use the Yamanuchi symbol  $y^{(i)}$  (see Ref. [43] for details) for a compact representation of the sequence of spin couplings in the  $3q$  states  $|s_1 s_2 (S_{12}) s_3 : S, \mu'\rangle_c$ ,

$$\begin{aligned} |[21]_S y_S^{(1)}, \mu'\rangle_c &= |\frac{1}{2} \frac{1}{2} (1) \frac{1}{2} : \frac{1}{2}, \mu'\rangle_c \\ |[21]_S y_S^{(2)}, \mu'\rangle_c &= |\frac{1}{2} \frac{1}{2} (0) \frac{1}{2} : \frac{1}{2}, \mu'\rangle_c, \end{aligned} \quad (4)$$

(the same notations are used for isospin states).

As usual the  $z$  axis is taken as the quantization axis both for the canonical ( $c$ ) and the front form ( $f$ ) spins. Here and further on, the symbols  $\mu'_i, \mu'_{12}, \mu'$  and  $\mu''_i, \mu''_{12}, \mu''$  denote the canonical spin projections on the  $z$  axis in initial and final states, respectively, while  $\mu_i, \mu_{12}, \mu$  and  $\bar{\mu}_i, \bar{\mu}_{12}, \bar{\mu}$  are the front form spin projections. Under the Melosh rotations (different for each quark with label  $i$ )

$$R_M^{(i)} |\frac{1}{2}, \mu'_i\rangle_c = \sum_{\mu_i} D_{\mu_i, \mu'_i}^{(\frac{1}{2})}(\theta_M^{(i)}) |\frac{1}{2}, \mu_i\rangle_f \quad (5)$$

the canonical spin basis functions (4) are transformed into the front form

$$\begin{aligned} \mathcal{R}_M |\frac{1}{2} \frac{1}{2} (S'_{12}) \frac{1}{2} : S', \mu'\rangle_c &= \sum_{S=1/2, 3/2} \sum_{S_{12}=0, 1} \\ &\times \sum_{\mu} C_{S_{12}, S'_{12}}^{SS'}(\mu, \mu') |\frac{1}{2} \frac{1}{2} (S_{12}) \frac{1}{2} : S, \mu\rangle_f. \end{aligned} \quad (6)$$

The coefficients  $C_{S_{12}, S'_{12}}^{SS'}(\mu, \mu')$  are the matrix elements of the triple product (2) of Melosh matrices (1) between the spin basis states in the  $3q$  system (4). Explicit expressions for the coefficients  $C_{S_{12}, S'_{12}}^{SS'}(\mu, \mu')$  are given in the Appendix. The coefficients  $C_{S_{12}, S'_{12}}^{SS'}$  depend on the relative momenta of quarks

$$\begin{aligned} \boldsymbol{\lambda}_{\perp} &= \frac{x_2 \mathbf{k}_{\perp 1} - x_1 \mathbf{k}_{\perp 2}}{x_1 + x_2}, \quad m = m_1 = m_2 = m_3, \\ \boldsymbol{\Lambda}_{\perp} &= \frac{x_3 (\mathbf{k}_{\perp 1} + \mathbf{k}_{\perp 2}) - (x_1 + x_2) \mathbf{k}_{\perp 3}}{x_1 + x_2 + x_3} = -\mathbf{k}_{\perp 3} \end{aligned} \quad (7)$$

and on the  $z^+$  components of the quark momenta,  $x_i = p_i^+ / P^+ = k_i^+ / \mathcal{M}_0$  with

$$x_1 = \xi \eta, \quad x_2 = \eta(1 - \xi), \quad x_3 = 1 - \eta, \quad (8)$$

where  $\{x_i, \mathbf{k}_{\perp i}\}$  is the LF momentum of the  $i$ th quark defined through the Lorentz transformation of the  $i$ th quark momentum to the rest frame of the  $3q$  system.

Note that the relative momentum  $\boldsymbol{\lambda}$  is odd with respect to the permutation  $P_{12}$  of the first and second quark while momentum  $\boldsymbol{\Lambda}$  is even

$$P_{12} \boldsymbol{\lambda}_{\perp} = -\boldsymbol{\lambda}_{\perp}, \quad P_{12} \boldsymbol{\Lambda}_{\perp} = \boldsymbol{\Lambda}_{\perp} \quad (9)$$

with  $P_{12} \xi = 1 - \xi$ ,  $P_{12} \eta = \eta$ . Thus the permutation symmetry of the resulting LF state (6) is not trivial and should be considered in detail.

In our case we have  $S' = \frac{1}{2}$  (the canonical nucleon spin), but after Melosh rotations of the quark spins this value transforms into two different values,  $S = \frac{1}{2}$  and  $\frac{3}{2}$ , which characterize the two different components of the nucleon wave function in the front form. For example, if we start from the canonical spin state  $|\frac{1}{2} \frac{1}{2} (0) \frac{1}{2} : \frac{1}{2}, \mu'\rangle_c$  [which possesses the fixed permutation symmetry  $[21]_S y_S^{(2)}$ ] we obtain the front-spin states with other values of  $S_{12}$  or  $S$ , e.g.  $S_{12} = 1$  and  $S = \frac{3}{2}$  [i.e. the states  $|[21]_S y_S^{(1)}, \mu'\rangle_f$  and  $|[3]_S, \mu'\rangle_f$ ] which supposedly violate the initial permutation symmetry of the  $3q$  system.

However, on the light front this does not lead to a violation of the Pauli exclusion principle. The reason for this is that the Melosh rotation of the spin state  $|[21]_S y_S^{(i)}, \mu\rangle_c$  turns into a superposition of combined spin-orbital ( $SP$ ) states  $|[21]_{PS} y_{PS}^{(j)}, \mu\rangle_f$  ( $j = 1, 2$ ) realized in the product space of spin ( $S$ ) and momentum ( $P$ ). The momentum-dependent factors of the coefficients  $C_{00}^{SS'}$  and  $C_{11}^{SS'}$  are even with respect to the permutation  $P_{12}$  while the coefficients  $C_{10}^{SS'}$  and  $C_{01}^{SS'}$  are odd. Hence, e.g. in the case

of  $C_{10}^{\frac{1}{2}\frac{1}{2}}$ , the term  $\sum_{\mu} C_{10}^{\frac{1}{2}\frac{1}{2}}(\mu, \mu') |[21]_S y_S^{(2)}, \mu'\rangle_f$  in Eq. (6) has the same value ( $y_{PS}^{(2)}$ ) of the Yamanuchi symbol in the (front)  $SP$  space as the initial value  $y_S^{(2)}$  in the (canonical)  $S$  space.

Using the coefficients  $C_{00}^{\frac{1}{2}\frac{1}{2}}$ ,  $C_{11}^{\frac{1}{2}\frac{1}{2}}$ ,  $C_{11}^{\frac{3}{2}\frac{1}{2}}$ ,  $C_{10}^{\frac{1}{2}\frac{1}{2}}$ ,  $C_{10}^{\frac{3}{2}\frac{1}{2}}$  and  $C_{01}^{\frac{1}{2}\frac{1}{2}}$  in Eq. (6) we obtain the correct basis vectors in the product space (the LF spin  $S$  and the LF momentum  $P$ ) for the irreducible representation (IR)  $[21]_{PS}$  of the permutation group  $S_3$

$$\begin{aligned} \mathcal{R}_M |[21]_S y_S^{(1)}, \mu'\rangle_c = \\ |[21]_{PS} y_{PS}^{(1)}, \mu'\rangle_f = \sum_{\mu} \left[ C_{01}^{\frac{1}{2}\frac{1}{2}}(\mu, \mu') \left| \frac{1}{2} \frac{1}{2} (0) \frac{1}{2} : \frac{1}{2}, \mu \right\rangle_f + \right. \\ \left. C_{11}^{\frac{1}{2}\frac{1}{2}}(\mu, \mu') \left| \frac{1}{2} \frac{1}{2} (1) \frac{1}{2} : \frac{1}{2}, \mu \right\rangle_f + C_{11}^{\frac{3}{2}\frac{1}{2}}(\mu, \mu') \left| \frac{1}{2} \frac{1}{2} (1) \frac{1}{2} : \frac{3}{2}, \mu \right\rangle_f \right] \end{aligned} \quad (10)$$

and

$$\begin{aligned} \mathcal{R}_M |[21]_S y_S^{(2)}, \mu'\rangle_c = \\ |[21]_{PS} y_{PS}^{(2)}, \mu'\rangle_f = \sum_{\mu} \left[ C_{00}^{\frac{1}{2}\frac{1}{2}}(\mu, \mu') \left| \frac{1}{2} \frac{1}{2} (0) \frac{1}{2} : \frac{1}{2}, \mu \right\rangle_f + \right. \\ \left. C_{10}^{\frac{1}{2}\frac{1}{2}}(\mu, \mu') \left| \frac{1}{2} \frac{1}{2} (1) \frac{1}{2} : \frac{1}{2}, \mu \right\rangle_f + C_{10}^{\frac{3}{2}\frac{1}{2}}(\mu, \mu') \left| \frac{1}{2} \frac{1}{2} (1) \frac{1}{2} : \frac{3}{2}, \mu \right\rangle_f \right] \end{aligned} \quad (11)$$

The result of the Melosh rotation of the basis state (3) can be written as a symmetric  $SU(6) \times O(3)$  basis state  $[3]_{PST}$  which satisfies the Pauli exclusion principle for the LF states:

$$\begin{aligned} \mathcal{R}_M |[3]_{ST}, \mu' t\rangle_c = \\ |[3]_{PST}, \mu' t\rangle_f = \sqrt{\frac{1}{2}} |[21]_{PS} y_{PS}^{(1)}, \mu'\rangle_f |[21]_T y_T^{(1)}, t\rangle \\ + \sqrt{\frac{1}{2}} |[21]_{PS} y_{PS}^{(2)}, \mu'\rangle_f |[21]_T y_T^{(2)}, t\rangle. \end{aligned} \quad (12)$$

Here we consider the Clebsch-Gordon combinations of quark LF spins

$$\begin{aligned} \left| \frac{1}{2} \frac{1}{2} (S_{12}) \frac{1}{2} : \frac{1}{2}, \mu \right\rangle_f = \sum_{\mu_{12}\mu_3} \sum_{\mu_1\mu_2} \left( \frac{1}{2} \mu_1 \frac{1}{2} \mu_2 | S_{12} \mu_{12} \right) \\ \times (S_{12} \mu_{12} \frac{1}{2} \mu_3 | \frac{1}{2} \mu) \left| \frac{1}{2} \mu_1 \right\rangle_f \left| \frac{1}{2} \mu_2 \right\rangle_f \left| \frac{1}{2} \mu_3 \right\rangle_f \end{aligned} \quad (13)$$

used in the right-hand sides of Eqs. (10) and (11). They are rather considered as basis vectors  $|[21]_{S_3} y_{S_3}^{(i)}, \mu\rangle$  of the IR  $[21]_{S_3}$  of the symmetric group  $S_3$  than the IR of the rotation group  $O(3)$  [or the spin group  $SU(2)_S$ ] which is not a kinematical subgroup for the LF dynamics. Fortunately, for three-particle systems the Clebsch-Gordon coefficients of the symmetric group  $S_3$  are the same as the Clebsch-Gordon coefficients of the rotation group  $O(3)$  [or the spin group  $SU(2)$ ] [43].

## B. Nucleon and Roper resonance wave functions

The spin-isospin part of the nucleon wave function is defined by Eq. (3) as a basis vector of the IR  $5\bar{6}$  ( $J^P = \frac{1}{2}^+$ ) of the  $SU(6)$  group. As a result of the Melosh rotation we obtained in Eq. (12) a relativistic representation of this state which depends on the light-front spin states defined in Eq. (13).

The full wave function also possesses a scalar factor  $\Phi_S(\mathcal{M}_0)$  — the analog of the radial part of nonrelativistic wave function. To preserve relativistic invariance the LF wave function  $\Phi_S$  should depend on the invariant mass of the system of initial quarks:

$$\mathcal{M}_0^2 \equiv \sum_{i=1}^3 \frac{m_i^2 + \mathbf{k}_{\perp i}^2}{x_i} = \frac{m^2 + \mathbf{\lambda}_{\perp}^2}{\eta \xi (1 - \xi)} + \frac{\eta m^2 + \mathbf{\Lambda}_{\perp}^2}{\eta (1 - \eta)} \quad (14)$$

The mass  $\mathcal{M}_0$  only depends on the square of relative momenta of quarks (7) and on the  $z^+$  components (8).

Note that in a special Breit frame where the momentum  $q^\mu$  transferred to the nucleon only has the transverse component  $\mathbf{q}_{\perp}$  (for definiteness the momentum  $\mathbf{q}_{\perp}$  is directed along the  $x$  axis),

$$q^\mu = \{0, \mathbf{q}_{\perp}, 0\}, \quad Q^2 = -q^2 = q_{\perp}^2, \quad q_{\perp} = |\mathbf{q}_{\perp}| \quad (15)$$

the quark relative momentum  $\mathbf{\lambda}_{\perp}$  is not changed, while the values of  $\mathbf{\Lambda}_{\perp}$  and  $\mathcal{M}_0$  become  $\mathbf{\Lambda}'_{\perp}$  and  $\mathcal{M}'_0$ , respectively, with

$$\mathbf{\Lambda}'_{\perp} = \mathbf{\Lambda}_{\perp} - \eta \mathbf{q}_{\perp}, \quad \mathcal{M}_0'^2 = \mathcal{M}_0^2 + \frac{\eta q_{\perp}^2 - 2 \mathbf{q}_{\perp} \cdot \mathbf{\Lambda}_{\perp}}{1 - \eta}. \quad (16)$$

Using Eqs. (10) and (11) we can write the nucleon wave function in the form

$$\begin{aligned} |N_{1/2+}(\mathcal{M}_0); \mu', t\rangle_f \\ = \Phi_S(\mathcal{M}_0) \left[ \sqrt{\frac{1}{2}} |[21]_{PS} y_{PS}^{(1)}, \mu'\rangle_f |[21]_T y_T^{(1)}, t\rangle \right. \\ \left. + \sqrt{\frac{1}{2}} |[21]_{PS} y_{PS}^{(2)}, \mu'\rangle_f |[21]_T y_T^{(2)}, t\rangle \right]. \end{aligned} \quad (17)$$

The Roper resonance wave function  $|N_{1/2+}^*, \mathcal{M}_0; \mu', t'\rangle$  has the same form, but now the function  $\Phi_S(\mathcal{M}_0)$  corresponds to a radial excitation of the nucleon. We further denote the nucleon function as  $\Phi_{0S}(\mathcal{M}_0)$  and use the notation  $\Phi_{2S}(\mathcal{M}_0)$  for the Roper resonance. In analogy to the harmonic oscillator model we define the radially excited wave function in the form

$$\Phi_{2S} = \mathcal{N}_{2S} \left( 1 - c_R \frac{\mathcal{M}_0^2}{\beta^2} \right) \Phi_{0S}, \quad (18)$$

where  $\beta$  is the scale parameter. Here the coefficient  $c_R$  can be determined by the orthogonality condition

$$\langle N_{1/2+}^*; \mu', t | N_{1/2+}; \mu', t \rangle = 0. \quad (19)$$

In the Breit frame (15) the initial nucleon has momentum  $-\frac{\mathbf{q}_\perp}{2}$  and the wave function (17) is denoted by  $|N_{1/2+}(\mathcal{M}_0, -\frac{\mathbf{q}_\perp}{2}; \mu', t)\rangle$ . The wave function of the final state  $|N'_{1/2+}(\mathcal{M}'_0, \frac{\mathbf{q}_\perp}{2}; \mu', t)\rangle$  corresponds to the momentum  $+\frac{\mathbf{q}_\perp}{2}$  and can be obtained from Eq. (17) by the substitutions  $\mathbf{\Lambda}_\perp \rightarrow \mathbf{\Lambda}'_\perp$  and  $\mathcal{M}_0 \rightarrow \mathcal{M}'_0$ .

### C. Matrix elements of the one-particle current

We now will have a look at the well-known basic formulas following Ref. [40]. We start with the electromagnetic current of a free quark considered as a Dirac particle with charge  $e_q$  and anomalous magnetic moment  $\kappa_q$  given as

$$j_q^\mu = e_q \left( \gamma^\mu + \frac{\kappa_q}{2m} i\sigma^{\mu\nu} q_\nu \right). \quad (20)$$

The  $z^+$  component of this current  $I_q^+ = j_q^0 + j_q^3$  plays a decisive role in the LF approach. As has been shown [40] in the special Breit frame (15), where  $q^0 = q^3 = 0$ , that the matrix element of any component of the one-particle current (20) can be expressed in terms of the  $I^+$  matrix element, provided that current conservation  $j^\mu q_\mu = 0$  is obeyed. Hence the nucleon form factors  $F_1$  (Dirac) and  $F_2$  (Pauli) can be calculated in terms of matrix elements of the  $I^+$  component of the current

$$I_q^{(i)+} = e_q^{(i)} \left( I f_1 - i\boldsymbol{\sigma}^{(i)} \cdot [\mathbf{z} \times \mathbf{q}_\perp] \frac{f_2}{2m} \right) \quad (21)$$

and

$$I_N^+ = e_N \left( I F_1 - i\boldsymbol{\sigma}_N \cdot [\mathbf{z} \times \mathbf{q}_\perp] \frac{F_2}{2m_N} \right) \quad (22)$$

written in the special Breit frame (15). In both cases the electric charge (without the factor  $e = \sqrt{4\pi\alpha}$ )

$$e_q^{(i)} = \frac{1}{6} + \frac{1}{2}\tau_3^{(i)}, \quad e_N = \frac{1}{2} + \frac{1}{2}\tau_{N3} \quad (23)$$

is included in the current. Quark form factors  $f_1$  and  $f_2$  could be included in addition, but here we consider the simplest variant without quark form factors ( $f_1=1, f_2=\kappa_q$ ) assuming that the quark is an elementary particle.

Current matrix elements between LF spin states

$$\begin{aligned} {}_f\langle \frac{1}{2}, \bar{\mu}_3 | I_q^{(3)+} | \frac{1}{2}, \mu_3 \rangle_f &= I_{\bar{\mu}_3 \mu_3}^{D+} + I_{\bar{\mu}_3 \mu_3}^{P+} \\ &= e_q^{(3)} \left[ \delta_{\bar{\mu}_3, \mu_3} + \delta_{\bar{\mu}_3, -\mu_3} (-1)^{1/2-\mu_3} \frac{q_\perp}{2m} \kappa_q \right] \end{aligned} \quad (24)$$

$$\begin{aligned} {}_f\langle N'_{1/2+}; \bar{\mu} | I_N^+ | N_{1/2+}; \mu \rangle_f \\ = e_N \left[ \delta_{\bar{\mu}, \mu} F_1 + \delta_{\bar{\mu}, -\mu} (-1)^{1/2-\mu} \frac{q_\perp}{2m_N} F_2 \right] \end{aligned} \quad (25)$$

have a momentum-independent Dirac part  $I_{\bar{\mu}_3 \mu_3}^{D+} = \delta_{\bar{\mu}_3 \mu_3}$  which only depends on the spin indices (for definiteness we take the quark number  $i=3$ ).

The canonical spin matrix elements for the electromagnetic transitions  $N + \gamma^* \rightarrow N'$  ( $N' = N, N^*$ ) are determined by the LF matrix element (25) using the following decomposition:

$$\begin{aligned} {}_c\langle N'_{1/2+}; \mu'', t | R_M^{(N)\dagger} I_N^+ R_M^{(N)} | N_{1/2+}; \mu', t \rangle_c \\ = \sum_{\bar{\mu}\mu} {}_c\langle N'_{1/2+}; \mu'' | R_M^{(N)\dagger} (\mu'', \bar{\mu}) | N'_{1/2+}; \bar{\mu} \rangle_f \\ \times {}_f\langle N'_{1/2+}; \bar{\mu}, t' | I_N^+ | N_{1/2+}; \mu, t \rangle_f \\ \times {}_f\langle N_{1/2+}; \mu | R_M^{(N)} (\mu, \mu') | N_{1/2+}; \mu' \rangle_c \end{aligned} \quad (26)$$

where (see, e.g., the first reference in Ref. [40])

$$R_M^{(N)}(\mu, \mu') = D_{\mu\mu'}^{(\frac{1}{2})}(\theta_M) \quad (27)$$

$$\cos \frac{\theta_M}{2} = \frac{1 + \sqrt{1 + \tau}}{\sqrt{(1 + \sqrt{1 + \tau})^2 + \tau}}, \quad \tau = \frac{Q^2}{4m_N^2}. \quad (28)$$

The observed nucleon electric and magnetic form factors are calculated with the matrix element (26).

Now we define the nucleon current as a sum of single-quark currents

$$I_{N(3q)}^+ = \sum_{j=1}^3 e_q^{(j)} I_q^{(j)+} \quad (29)$$

and calculate the nucleon Dirac/Pauli form factors with the quark wave functions defined in Eq. (17). For  $F_1$  and  $F_2$  we use the following definitions (see Refs. [19, 41, 42] for details)

$$\begin{aligned} F_1 &= \frac{1}{2} \sum_{\mu'\mu''} \delta_{\mu', \mu''} \\ &\times {}_c\langle N'_{1/2+}; \mu'', t | \mathcal{R}_M^\dagger I_{N(3q)}^+ \mathcal{R}_M | N_{1/2+}; \mu', t \rangle_c, \\ F_2 &= \frac{1}{2} \sum_{\mu'\mu''} \delta_{\mu', -\mu''} (-1)^{\frac{1}{2}-\mu'} \\ &\times {}_c\langle N'_{1/2+}; \mu'', t | \mathcal{R}_M^\dagger I_{N(3q)}^+ \mathcal{R}_M | N_{1/2+}; \mu', t \rangle_c. \end{aligned} \quad (30)$$

Here  $\mathcal{R}_M$  is the three-quark Melosh rotation defined in Eqs. (1)-(2). Further on the standard relation between the Sachs and Dirac/Pauli form factors

$$G_E = F_1 - \tau F_2, \quad G_M = F_1 + F_2 \quad (31)$$

can be used.

### D. Form factors in terms of the single-quark current

To calculate the nucleon form factors  $F_1, F_2$  when starting from the LF quark current (24) we define the nucleon matrix element (26) in terms of the quark wave

function (17) deduced in Sec. II B. The definition of the quark matrix element implies integration over the wave functions involving the six-dimensional momentum space

$$\begin{aligned} & {}_c\langle N'_{1/2+}, \frac{\mathbf{q}_\perp}{2}; \mu'', t | \mathcal{R}_M^\dagger I_{N(3q)}^+ \mathcal{R}_M | N_{1/2+}, -\frac{\mathbf{q}_\perp}{2}; \mu', t \rangle_c \\ &= \frac{\mathcal{N}_p}{(2\pi)^6} \int_0^1 d\xi \int_0^1 d\eta \int d^2\mathbf{\Lambda}_\perp \int d^2\mathbf{\lambda}_\perp J(\xi, \eta, \mathbf{\Lambda}_\perp, \mathbf{\lambda}_\perp) \\ & \times 3 \langle N'_{1/2+}(\mathcal{M}'_0); \mu'', t | I_q^{(3)+} | N_{1/2+}(\mathcal{M}_0); \mu', t \rangle. \end{aligned} \quad (32)$$

The integrand in Eq. (32) includes the combinatorial factor 3 (the number of quarks in the system) and the Jacobian  $J$  which corresponds to the transition from ordinary quark momenta  $\mathbf{k}_1, \mathbf{k}_2, \mathbf{k}_s$  to the relative LF variables (7) and (8)

$$J(\xi, \eta, \mathbf{\Lambda}_\perp, \mathbf{\lambda}_\perp) = \frac{P^+}{P'^+} \frac{\sqrt{\prod_{i=1}^3 \omega_i \prod_{j=1}^3 \omega'_j}}{\xi(1-\xi)\eta(1-\eta)\sqrt{\mathcal{M}_0\mathcal{M}'_0}} \quad (33)$$

Here a standard definition for the  $i$ th quark energy  $\omega_i$  is used

$$\begin{aligned} \omega_i &= \frac{1}{2} \left( \mathcal{M}_0 x_i + \frac{m^2 + \mathbf{k}_{\perp i}^2}{\mathcal{M}_0 x_i} \right), \quad \mathbf{k}_{\perp 1} = \mathbf{\lambda}_\perp + \xi \mathbf{\Lambda}_\perp, \\ \mathbf{k}_{\perp 2} &= -\mathbf{\lambda}_\perp + (1-\xi)\mathbf{\Lambda}_\perp, \quad \mathbf{k}_{\perp 3} = -\mathbf{\Lambda}_\perp \end{aligned} \quad (34)$$

while the notation  $\omega'_j$  is reserved for the energy of  $j$ th quark in the final state [then the substitutions  $\mathbf{k}_{\perp i} \rightarrow \mathbf{k}'_{\perp j}$ ,  $\mathbf{\Lambda}_\perp \rightarrow \mathbf{\Lambda}'_\perp$  and  $\mathcal{M}_0 \rightarrow \mathcal{M}'_0$  should be made in Eq. (34)]. The matrix element (32) is normalized with the factor  $\mathcal{N}_p$  which provides the correct proton charge of unity, i.e  $F_{1p}(0) = 1$ .

The integrand in Eq. (32) consists of two components which originate from the Dirac ( $D$ ) and Pauli ( $P$ ) terms of the quark current of Eq. (24). For the Dirac component of the integrand we use the representation

$$\begin{aligned} \mathcal{J}_{\mu''\mu'}^D(\mathcal{M}'_0, \mathcal{M}_0; t) &= 3 \langle N'_{1/2+}(\mathcal{M}'_0); \mu'', t | \sum_{\mu_3 \bar{\mu}_3} |\frac{1}{2}, \bar{\mu}_3\rangle \langle \frac{1}{2}, \bar{\mu}_3| \\ & \times I_{\mu_3 \mu_3}^{D+} |\frac{1}{2}, \mu_3\rangle \langle \frac{1}{2}, \mu_3| N_{1/2+}(\mathcal{M}_0); \mu', t \rangle \end{aligned} \quad (35)$$

and the same formula with the substitution  $I_{\mu_3 \mu_3}^{D+} \rightarrow I_{\mu_3 \mu_3}^{P+} = (\kappa_q q_\perp / 2m) \delta_{\bar{\mu}_3, -\mu_3} (-1)^{1/2-\mu_3}$  is used for the Pauli component  $\mathcal{J}_{\mu''\mu'}^P(\mathcal{M}'_0, \mathcal{M}_0; t)$ .

It is rather straightforward to derive explicit expressions for  $\mathcal{J}_{\mu''\mu'}^D$  and  $\mathcal{J}_{\mu''\mu'}^P$  in terms of the coefficients  $C_{S_{12}, S'_{12}}^{SS'}$  when the wave functions  $|N_{1/2+}(\mathcal{M}_0); \mu', t\rangle$  and  $|N'_{1/2+}(\mathcal{M}'_0); \mu'', t\rangle$  are substituted in the form given in Eq. (17) with the basis vectors (10) and (11) defined in

Sec. II A. The result is

$$\begin{aligned} \mathcal{J}_{\mu''\mu'}^D(\mathcal{M}'_0, \mathcal{M}_0; t) &= 3\Phi_{S'}(\mathcal{M}'_0)\Phi_S(\mathcal{M}_0) \frac{1}{2} \sum_{\mu\bar{\mu}} \delta_{\mu\bar{\mu}} \\ & \times \{ [C'_{01}^*(\bar{\mu}, \mu'') C_{01}(\mu, \mu') + C'_{11}^*(\bar{\mu}, \mu'') C_{11}(\mu, \mu')] e_1(t) \\ & + [C'_{00}^*(\bar{\mu}, \mu'') C_{00}(\mu, \mu') + C'_{10}^*(\bar{\mu}, \mu'') C_{10}(\mu, \mu')] e_2(t) \}, \end{aligned} \quad (36)$$

$$\begin{aligned} \mathcal{J}_{\mu''\mu'}^P(\mathcal{M}'_0, \mathcal{M}_0; t) &= 3\Phi_{S'}(\mathcal{M}'_0)\Phi_S(\mathcal{M}_0) \frac{1}{2} \frac{\kappa_q q_\perp}{2m} \sum_{\mu\bar{\mu}} A_{\bar{\mu}, \mu} \\ & \times \{ [C'_{01}^*(\bar{\mu}, \mu'') C_{01}(\mu, \mu') + C'_{11}^*(\bar{\mu}, \mu'') C_{11}(\mu, \mu')] e_1(t) \\ & + [C'_{00}^*(\bar{\mu}, \mu'') C_{00}(\mu, \mu') + C'_{10}^*(\bar{\mu}, \mu'') C_{10}(\mu, \mu')] e_2(t) \}, \end{aligned} \quad (37)$$

where the matrix  $A_{\bar{\mu}, \mu}$  is given in the Appendix and each term  $C'_{S_{12}S'_{12}}(\bar{\mu}, \mu'') C_{S_{12}S'_{12}}(\mu, \mu')$  in the rhs of Eqs. (36) and (37) is a symbolical expression that implies a sum of two terms for the front spins  $S = \frac{1}{2}$  and  $\frac{3}{2}$  as it follows from Eqs. (10) and (11), e.g.,

$$\begin{aligned} C'_{11}^*(\bar{\mu}, \mu'') C_{11}(\mu, \mu') &\doteq \\ & C_{11}^{\frac{1}{2}\frac{1}{2}*}(\mathbf{\lambda}_\perp, \mathbf{\Lambda}'_\perp; \bar{\mu}, \mu'') C_{11}^{\frac{1}{2}\frac{1}{2}}(\mathbf{\lambda}_\perp, \mathbf{\Lambda}_\perp; \mu, \mu') \\ & + C_{11}^{\frac{3}{2}\frac{1}{2}*}(\mathbf{\lambda}_\perp, \mathbf{\Lambda}'_\perp; \bar{\mu}, \mu'') C_{11}^{\frac{3}{2}\frac{1}{2}}(\mathbf{\lambda}_\perp, \mathbf{\Lambda}_\perp; \mu, \mu') \end{aligned} \quad (38)$$

In Eqs. (36) and (37) the isospin factors are

$$\begin{aligned} e_1(t) &= \\ \langle [21]_T y_T^{(1)}, t | e_q^{(3)} | [21]_T y_T^{(1)}, t \rangle &= \begin{cases} 0, & t = +\frac{1}{2}, \\ \frac{1}{3}, & t = -\frac{1}{2} \end{cases} \end{aligned} \quad (39)$$

$$\begin{aligned} e_2(t) &= \\ \langle [21]_T y_T^{(2)}, t | e_q^{(3)} | [21]_T y_T^{(2)}, t \rangle &= \begin{cases} \frac{2}{3}, & t = +\frac{1}{2}, \\ -\frac{1}{3}, & t = -\frac{1}{2} \end{cases} \end{aligned} \quad (40)$$

In the following  $F_{1t}^D$  and  $F_{1t}^P$  denote the contributions of the Dirac and Pauli quark currents  $I_{\bar{\mu}_3 \mu_3}^{D+}$  and  $I_{\bar{\mu}_3 \mu_3}^{P+}$  to the nucleon  $F_1$  form factor:  $F_{1t} = F_{1t}^D + F_{1t}^P$ , while the same notations are used for the nucleon  $F_2$  form factor:  $F_{2t} = F_{2t}^D + F_{2t}^P$ . These contributions to  $F_{1t}(F_{2t})$  are represented by the following six-dimensional integrals of the functions defined in Eqs. (36) and (37) with

$$F_{1t}^D = \int d\mathcal{V}_{LF} \frac{1}{2} \sum_{\mu'\mu''} \delta_{\mu', \mu''} \mathcal{J}_{\mu''\mu'}^D(\mathcal{M}'_0, \mathcal{M}_0; t) \quad (41)$$

$$\begin{aligned} F_{2t}^D &= \int d\mathcal{V}_{LF} \frac{1}{2} \sum_{\mu'\mu''} \delta_{\mu', -\mu''} (-1)^{1/2-\mu'} \\ & \times \frac{2m_N}{q_\perp} \mathcal{J}_{\mu''\mu'}^D(\mathcal{M}'_0, \mathcal{M}_0; t) \end{aligned} \quad (42)$$

$$F_{1t}^P = \int d\mathcal{V}_{LF} \frac{1}{2} \sum_{\mu'\mu''} \delta_{\mu',\mu''} \mathcal{J}_{\mu''\mu'}^P(\mathcal{M}'_0, \mathcal{M}_0; t) \quad (43)$$

$$F_{2t}^P = \int d\mathcal{V}_{LF} \frac{1}{2} \sum_{\mu'\mu''} \delta_{\mu',-\mu''} (-1)^{1/2-\mu'} \times \frac{2m_N}{q_\perp} \mathcal{J}_{\mu''\mu'}^P(\mathcal{M}'_0, \mathcal{M}_0; t). \quad (44)$$

Here we denote the integration volume in compact form as

$$d\mathcal{V}_{LF} = J(\xi, \eta, \Lambda_\perp, \lambda_\perp) d\xi d\eta d^2\Lambda_\perp d^2\lambda_\perp.$$

### III. DESCRIPTION OF DATA ON FORM FACTORS AND HELICITY AMPLITUDES

#### A. Nucleon form factors

Previous results enable us to determine the nucleon form factors in a wide  $Q^2$  range from 0 to 35 GeV<sup>2</sup>. The nucleon form factors  $F_1/F_2$  are defined as the sums of matrix elements (41)–(44) of the Dirac/Pauli quark currents

$$F_{1t} = F_{1t}^D + F_{1t}^P, \quad F_{2t} = F_{2t}^D + F_{2t}^P \quad (45)$$

where  $t = +1/2$  (proton),  $t = -1/2$  (neutron). The Sachs form factors  $G_E/G_M$  are defined by Eq. (31).

In the LF approaches [18, 19, 28, 41] the “radial” part of the  $S$ -wave quark core of the nucleon is usually described by the Gaussian  $\Phi_{0S} = \mathcal{N}_{0S} \exp(-\mathcal{M}_0^2/2\beta^2)$ . However, for large  $Q^2$  the elastic or inelastic form factors are suppressed by the Gaussian, hence the pQCD prediction for their asymptotic behavior with  $G_E \sim 1/Q^4$ ,  $G_M \sim 1/Q^6$  cannot be provided.

A superposition of several harmonic oscillator wave functions (up to 20) was used in more advanced approaches [19, 25] to obtain a realistic description of form factors at low and moderate values of  $Q^2$ . Nevertheless, the problem of the asymptotic power behavior of nucleon form factors can only be solved in such models where many free parameters are available to be fitted to the data up to high values of  $Q^2$ .

Recently, in Ref. [28], a running quark mass [in the pole form  $m(Q^2) = m(0)/(1 + Q^2/\Lambda^2)$ ] was used in the LF model with a Gaussian shaped wave function. This model is consistent (at least qualitatively) with the QCD prediction for the  $Q^2$  behavior of the quark mass. The problem is essentially as follows: in quark models the factor  $m^{-1}(Q^2)$  appears in the expression for the nucleon form factor  $F_2$ . Therefore, the falloff of the Gaussian in  $F_2$  at large  $Q^2$  can be compensated by an increase in  $m^{-1}(Q^2)$ . As a result a realistic description of the  $Q^2$  behavior of both the nucleon form factors and the Roper resonance production helicity amplitudes was obtained in Ref. [28].

Here we suggest an alternative method for solving the problem of the “non-Gaussian behavior” of form factors at large  $Q^2$ . In our opinion a pole form of the nucleon/Roper wave function

$$\Phi_{0S} = \mathcal{N}_{0S} \frac{1}{(1 + \mathcal{M}_0^2/\beta^2)^\gamma} \quad (46)$$

is also workable and correlates well with QCD predictions for the high  $Q^2$  behavior of elastic and inelastic form factors. Two decades ago such a pole form for the nucleon wave function was considered in Ref. [42]. A realistic description of nucleon form factors and of magnetic moments was obtained for a value of  $\gamma = 3.5$ . At this time the theoretical description of data on  $G_E$ ,  $G_M$  was rather reasonable; the case of the Roper resonance was not discussed because of the absence of good data. Now a large set of new high-quality data both on the nucleon form factors [44, 45, 47–53, 55, 58, 64] and on the electroproduction of the Roper resonance [1–3] are available. Hence a precise analysis in terms of a common approach both to elastic and inelastic form factors is possible now..

Here we show that the given LF quark model allows for a good description of all the new data on nucleon form factors in a large interval of  $Q^2$  from 0 up to 35 GeV<sup>2</sup>. The model has only five free parameters [see Eqs. (20) and (46)],  $\gamma$ ,  $\beta$ ,  $m$ , and  $\varkappa_q$ , which are fitted to the data. For the values

$$\gamma = 3.51, \quad \beta = 0.579 \text{ GeV}, \quad m = 0.251 \text{ GeV}, \\ \varkappa_u = -0.017, \quad \varkappa_d = 0.0295 \quad (47)$$

an optimal description of the elastic nucleon data is obtained (see Figs. 1–8). We present a comparison with known data and the soft-wall AdS/QCD approach [33], where elastic nucleon form factors and nucleon-Roper transition form factors have been analyzed in detail. The model generates a  $Q^2$  behavior for  $Q^4 F_{1p}(Q^2)$ ,  $Q^4 F_{1n}(Q^2)$  and  $Q^2 F_{2p}(Q^2)/F_{1p}(Q^2)$  which should tend to a constant at high  $Q^2$  (see Figs. 1, 2 and 3). At low and moderate values of  $Q^2$  the model is compatible not only with the magnetic moments of the nucleons,  $\mu_p = F_{1p}(0) + F_{2p}(0) = 2.79$  and  $\mu_n = F_{1n}(0) + F_{2n}(0) = -1.91$  but also with the known negative slope for the ratio  $G_E^p(Q^2)/G_M^p(Q^2)$  (Fig. 4). The absolute theory values for  $G_M^p(Q^2)$ ,  $G_M^n(Q^2)$  and  $G_E^p(Q^2)$  do also correlate well with the data as evident from Figs. 5, 6 and 7, respectively, where the dipole form factor  $G_D = (1 + Q^2/0.71)^{-2}$  is used as a common denominator.

Only in the case of the neutron charge form factor  $G_E^n$  (Fig. 8) this model is not entirely adequate to describe data at low and intermediate values of  $Q^2$ . But in this  $Q^2$  region the pion cloud contribution to  $G_E^n$ , neglected in the present work, can be considerable. This contribution can also be important for inelastic nucleon form factors at  $Q^2 \lesssim 1 \text{ GeV}^2$ , as was recently noted in Ref. [28]. In our recent work [35] we also pointed out the role of the pion cloud in the electroproduction of the Roper resonance.

## B. Helicity amplitudes in the electroexcitation of the Roper resonance

As was suggested in Refs. [28, 35] the  $\sigma$  meson along with the pion cloud can contribute significantly to the process  $p + \gamma^* \rightarrow R$ . In Ref. [35] we considered the contribution of the  $\sigma$  to the electroproduction of the Roper resonance by assuming a composite structure. In this case the Roper resonance is set up as a superposition of the radially excited three-quark configuration  $3q^*$  and the hadron molecule component  $N + \sigma$  as

$$|R\rangle = \cos\theta|3q^*\rangle + \sin\theta|N + \sigma\rangle. \quad (48)$$

A mixing angle  $\theta$  is introduced:  $\cos^2\theta$  and  $\sin^2\theta$  represent the probabilities to find a  $3q^*$  and hadronic configuration, respectively. The parameter  $\theta$  was adjusted to optimize the description of the electroproduction data resulting in the optimal value of  $\cos\theta = 0.8$  [35].

In Ref. [35] the contribution of a hadronic  $N + \sigma$  component to the process  $p + \gamma^* \rightarrow R$  was calculated in the framework of a relativistic approach; the related technique was proposed and extensively used in Ref. [80]. The interaction vertices of these diagrams are derived using nonlocal relativistic Lagrangians with  $NN\sigma$  and  $NR\sigma$  couplings, which are manifestly gauge invariant.

But at the same time a somewhat inconsistent (non-relativistic) technique was used for the quarks. The contribution of the nucleon quark core to the transition  $3q + \gamma^* \rightarrow 3q^*$  was calculated in terms of a nonrelativistic quark shell model with Gaussian wave functions. Here we remedy this original defect and recalculate the quark amplitudes with the quark LF wave functions of the nucleon, Eq. (46), and the Roper resonance, Eq. (18).

The transverse and longitudinal helicity amplitudes  $A_{1/2}$  and  $S_{1/2}$  for the electroproduction of the Roper resonance are defined (see, e.g. Ref. [81]) by matrix elements of the hadronic current  $J^\mu$ . These matrix elements

$$\begin{aligned} \langle R(p', \lambda') | J^\mu(0) | N(p, \lambda) \rangle \\ = \bar{u}_R(p', \lambda') \left\{ F_1^{RN}(Q^2) \left( \gamma^\mu - \not{q} \frac{q^\mu}{Q^2} \right) \right. \\ \left. + F_2^{RN}(Q^2) \frac{i\sigma^{\mu\nu} q_\nu}{m_R + m_N} u_N(p, \lambda) \right\} \end{aligned} \quad (49)$$

are taken between the helicity states of the initial nucleon  $|N(p, \lambda)\rangle$  and the final Roper resonance  $|R(p', \lambda')\rangle$  (we use notations and definitions given in Ref. [81], where formulas are written in the rest frame of the Roper resonance) with

$$A_{1/2} = -\sqrt{\frac{\pi\alpha}{2k_R m_R m_N}} \langle R(p', \frac{1}{2}) | \mathbf{J} \cdot \boldsymbol{\epsilon}_{\lambda=+1} | N(p, -\frac{1}{2}) \rangle \quad (50)$$

$$S_{1/2} = -\sqrt{\frac{\pi\alpha}{2k_R m_R m_N}} \langle R(p', \frac{1}{2}) | J^0 | N(p, \frac{1}{2}) \rangle \quad (51)$$

where  $k_R = (m_R^2 - m_N^2)/(2m_R)$  and the transverse polarization vector is  $\{\boldsymbol{\epsilon}_{\lambda=+1}\} = -\sqrt{\frac{1}{2}}\{1, i, 0\}$ .

It follows from Eqs. (49)–(51) that the amplitudes  $A_{1/2}$  and  $S_{1/2}$  can be expressed in terms of the invariant form factors  $F_1^{RN}(Q^2)$  and  $F_2^{RN}(Q^2)$  for which we already have explicit expressions (41)–(45) in the LF formalism. We have the relations

$$A_{1/2} = \sqrt{\frac{\pi\alpha}{k_R m_R m_N}} Q_- (F_1^{RN} + F_2^{RN}), \quad (52)$$

$$\begin{aligned} S_{1/2} = \sqrt{\frac{\pi\alpha}{2k_R m_R m_N}} \frac{Q_+ Q_-}{Q^2} \frac{m_R + m_N}{2m_R} \\ \times Q_- \left( F_1^{RN} - \frac{Q^2}{(m_R + m_N)^2} F_2^{RN} \right), \end{aligned} \quad (53)$$

where  $Q_\pm = \sqrt{(m_R \pm m_N)^2 + Q^2}$ .  $F_1^{RN}(Q^2)$  and  $F_2^{RN}(Q^2)$  are given by Eqs. (41)–(45) with the wave functions  $\Phi_S = \Phi_{0S}$  (for the initial nucleon) and  $\Phi_{S'} = \Phi_{2S}$  (for the final Roper resonance).

The calculated helicity amplitudes  $A_{1/2}$  and  $S_{1/2}$  are shown in Fig. 9 for unchanged values of the model parameters, Eq. (47), previously fitted to the nucleon data. The only additional free parameter is the mixing angle  $\theta$  of Eq. (48). We vary  $\cos\theta$  from 0.7 to 1 where results for the specific values  $\cos\theta = 1$  and 0.7 are shown in Fig. 9. When the Roper wave function corresponds to a  $3q^*$  state ( $\cos\theta = 1$ ) predictions for both helicity amplitudes  $A_{1/2}$  and  $S_{1/2}$  (dashed lines) are much too large in comparison with the data [1, 2]. A value of about  $\cos\theta = 0.7$  (solid lines) is preferred in the present model where data for  $Q^2 \lesssim 2 \text{ GeV}^2$  of both helicity amplitudes can be roughly reproduced. For  $Q^2$  in the range from 2 to 4  $\text{GeV}^2$  the behavior of the  $A_{1/2}$  data cannot be explained sufficiently. Note that in our previous nonrelativistic model [35] (dashed dotted lines in Fig. 9) a better description of the data was achieved with an optimal value of  $\cos\theta = 0.8$ .

For comparison we also show in Fig. 9 the results of Ref. [28] for the LF model with running quark masses (the double-dotted dashed line). The weight of the three-quark core in the Roper wave function in that model of  $\cos\theta = 0.73$  is very close to the value  $\cos\theta = 0.7$  deduced in our model. Both predictions have a similar behavior for  $A_{1/2}$  at low and intermediate values of  $Q^2 \lesssim 4\text{--}5 \text{ GeV}^2$  but at higher  $Q^2$  the predictions increase relative to present data. On the basis of the CLAS data at intermediate  $Q^2 \lesssim 4\text{--}5 \text{ GeV}^2$  both models point to the same (about 50%) probability for the  $3q$  component in the wave function of the Roper resonance. We can conclude that the quark LF model might represent a viable approach to the description of the data at high  $Q^2$  if the  $3q^*$  component in the Roper resonance is subleading, maximally with a probability of not even 50%. The remaining structure is dominated by more complicated soft components: the meson cloud or  $q\bar{q}$ ,  $qq\bar{q}\bar{q}$ , etc. states. The contribution of these configurations to form factors becomes

negligible with growing  $Q^2$ . Soft components can also modify the  $Q^2$  behavior of the helicity amplitudes at low and moderate values of  $Q^2$ , while in the high  $Q^2$  region the  $3q^*$  core defines the power asymptotics of the amplitudes predicted by pQCD.

#### IV. SUMMARY

We presented a version of the light-front approach to elastic and inelastic nucleon form factors in which the LF three-quark configurations (obtained with the Melosh rotation of the canonical spin states  $|s_1 s_2 (S_{12}) s_3 : S, \mu\rangle_c$ ) satisfy the Pauli exclusion principle on the LF. Such an approach is equivalent to a variant where configuration mixing on the LF is neglected, but it appears to be a good approximation at least for nucleons. Both  $N + \gamma^* \rightarrow N$  and  $N + \gamma^* \rightarrow N^*$  transition amplitudes are described in a common framework based on a relativistic quark model satisfying the Pauli exclusion principle on the LF.

A pole form for the “radial” part of the nucleon wave function allows for a good description of the nucleon form factors in a large  $Q^2$  region from  $Q^2 = 0$  (proton and neutron magnetic moments) to high values of about 30  $\text{GeV}^2$  (with the power behavior  $\sim Q^{-4}$ ,  $\sim Q^{-6}$  for  $G_E$ ,  $G_M$ ). At the same time the calculated helicity amplitudes  $A_{1/2}(Q^2)$  and  $S_{1/2}(Q^2)$  of electroproduction of the Roper resonance on the proton occur to be too large in comparison with recent data at low and moderate values of  $Q^2$ . A closer description of both  $A_{1/2}(Q^2)$  and  $S_{1/2}(Q^2)$  amplitudes can only be obtained if the quark core configuration in the Roper resonance is sup-

pressed. The remaining part of the full  $N^*$  state could be a soft component which is described in terms of a meson cloud or equivalently in terms of a soft cloud of  $q\bar{q}$ ,  $(qq)(\bar{q}\bar{q})$ , ... etc. pairs.

In a first approximation we assume that this soft component can be described by a hadronic molecular  $N + \sigma$  state, the inner structure of which we have studied in our recent work [35]. Our evaluation shows that the contribution of such a component to the inelastic  $N \rightarrow R$  form factors  $F_1^{RN}(Q^2)$  and  $F_2^{RN}(Q^2)$  becomes negligible with growing  $Q^2$ . The asymptotic  $Q^2$  behavior of  $F_1^{RN}$  and  $F_2^{RN}$  is given by the quark core component  $3q^*$  resulting in a true power law and with a reduced absolute value of the amplitude (about 50% compared to the full  $3q \rightarrow 3q^*$  amplitude). At low and moderate values of  $Q^2$  the hadronic molecule component improves the description of the form factors. At this level the considered model is too simple to provide strong evidence for a large hadronic  $N + \sigma$  component which effectively represents the soft part of the full wave function.

#### Acknowledgments

This work was supported by the DFG under Contracts No. FA67/39-1 and No. LY 114/2-1. The work is done partially under Project No. 2.3684.2011 of Tomsk State University. V. E. L. would like to thank Institute of Nuclear Physics, Moscow State University, Russia and Tomsk Polytechnic University, Russia for warm hospitality.

- 
- [1] I. G. Aznauryan *et al.* (CLAS Collaboration), Phys. Rev. C **80**, 055203 (2009).
  - [2] V. I. Mokeev *et al.* (CLAS Collaboration) Phys. Rev. C **86**, 035203 (2012); V. I. Mokeev, V. D. Burkert, T. S. H. Lee, L. Elouadrhiri, G. V. Fedotov and B. S. Ishkhanov (CLAS Collaboration), Phys. Rev. C **80**, 045212 (2009).
  - [3] A. V. Sarantsev *et al.* (CB-ELSA Collaboration and A2-TAPS Collaboration), Phys. Lett. B **659**, 94 (2008); A. V. Sarantsev, in 8th International Workshop on the Physics of Excited Nucleons, NSTAR2011, Jefferson Laboratory, Newport News, VA, May 2011.
  - [4] K. Nakamura *et al.* (Particle Data Group), J. Phys. G **37**, 075021 (2010).
  - [5] P. O. Bowman *et al.*, Phys. Rev. D **71**, 054507 (2005); S. Boinpolly *et al.*, Int. J. Mod. Phys. **22**, 5053 (2007).
  - [6] G. P. Engel, C. B. Lang, M. Limmer, D. Mohler, and A. Schafer, Phys. Rev. D **82**, 034505 (2010).
  - [7] V. M. Braun *et al.*, Phys. Rev. Lett. **103**, 072001 (2009); V. M. Braun, A. Lenz, and M. Wittmann, Phys. Rev. D **73**, 094019 (2006).
  - [8] C. D. Roberts and G. Williams, Prog. Part. Nucl. Phys. **33**, 477 (1994); P. Maris and C. D. Roberts, Int. J. Mod. Phys., E **12**, 297 (2003); R. Alkofer and L. von Smekal, Phys. Rep. **353**, 281 (2001).
  - [9] I. C. Cloët, C. D. Roberts, and D. J. Wilson, AIP Conf. Proc. **1388**, 121 (2011).
  - [10] H. L. L. Roberts, L. Chang, I. C. Cloët, and C. D. Roberts, Few-Body Syst. **51**, 1 (2011).
  - [11] N. Suzuki *et al.*, Phys. Rev. Lett. **104**, 042302 (2010).
  - [12] A. Matsuyama, T. Sato, and T. S. H. Lee, Phys. Rep. **439**, 193 (2007).
  - [13] N. Suzuki, T. Sato, and T. S. H. Lee, Phys. Rev. C **79**, 025205 (2009); N. Suzuki, B. Julia-Diaz, H. Kamano, T. S. H. Lee, A. Matsuyama, and T. Sato, Phys. Rev. Lett. **104**, 042302 (2010); B. Julia-Diaz, T. S. H. Lee, A. Matsuyama and T. Sato, Phys. Rev. C **76**, 065201 (2007); J. Liu, R. D. McKeown and M. J. Ramsey-Musolf, Phys. Rev. C **76**, 025202 (2007).
  - [14] O. Krehl, C. Hanhart, C. Krewald and J. Speth, Phys. Rev. C **62**, 025207 (2000); M. Döring, C. Hanhart, F. Huang, S. Krewald and U.-G. Meissner, Phys. Lett. B **681**, 26 (2009).
  - [15] M. B. Gavelle, A. Le Yaouanc, L. Oliver, O. Pene, J. C. Raynal, and S. Sood, Phys. Rev. D **21**, 182 (1980).
  - [16] Z.-P. Li, V. Burkert, and Z.-J. Li, Phys. Rev. D **46**, 70 (1992).
  - [17] F. E. Close and Z. P. Li, Phys. Rev. D **42**, 2194 (1990).

- [18] S. Capstick and B. D. Keister, Phys. Rev. D **51**, 3598 (1995).
- [19] F. Cardarelli, E. Pace, G. Salme, and D. Simula, Nucl. Phys. **A623**, 361c (1997); Phys. Lett. B **371**, 7 (1996).
- [20] I. G. Aznauryan, Phys. Rev. C **76**, 025212 (2007).
- [21] F. Cano and P. Gonzalez, Phys. Lett. B **431**, 270 (1998).
- [22] Q. B. Li and D. O. Riska, Phys. Rev. C **74**, 015202 (2006).
- [23] V. D. Burkert and T. S. H. Lee, Int. J. Mod. Phys. E **13**, 1035 (2004).
- [24] I. G. Aznauryan and V. D. Burkert, Prog. Part. Nucl. Phys. **67**, 1 (2012).
- [25] S. Capstick, B. D. Keister, and D. Morel, J. Phys. Conf. Ser. **69**, 012016 (2007).
- [26] G. Ramalho and K. Tsushima, Phys. Rev. D **81**, 074020 (2010).
- [27] B. Golli, S. Sirca, and M. Fiolhais, Eur. Phys. J. A **42**, 185 (2009).
- [28] I. G. Aznauryan and V. D. Burkert, Phys. Rev. C **85**, 055202 (2012).
- [29] G. F. de Teramond and S. J. Brodsky, AIP Conf. Proc. **1432**, 168 (2012).
- [30] T. Gutsche, V. E. Lyubovitskij, I. Schmidt, and A. Vega, Phys. Rev. D **87**, 016017 (2013).
- [31] T. Gutsche, V. E. Lyubovitskij, I. Schmidt, and A. Vega, Phys. Rev. D **85**, 076003 (2012); A. Vega, I. Schmidt, T. Gutsche, and V. E. Lyubovitskij, Phys. Rev. D **83**, 036001 (2011).
- [32] T. Branz, T. Gutsche, V. E. Lyubovitskij, I. Schmidt, and A. Vega, Phys. Rev. D **82**, 074022 (2010); A. Vega, I. Schmidt, T. Branz, T. Gutsche and V. E. Lyubovitskij, Phys. Rev. D **80**, 055014 (2009); T. Gutsche, V. E. Lyubovitskij, I. Schmidt and A. Vega, Phys. Rev. D **87**, 056001 (2013).
- [33] T. Gutsche, V. E. Lyubovitskij, I. Schmidt and A. Vega, Phys. Rev. D **86**, 036007 (2012).
- [34] H. Kamano, AIP Conf. Proc. **1374**, 501 (2011).
- [35] I. T. Obukhovskiy, A. Faessler, D. K. Fedorov, T. Gutsche, and V. E. Lyubovitskij, Phys. Rev. D **84**, 014004 (2011).
- [36] S. Capstick *et al.*, Eur. Phys. J. A **35**, 253 (2008).
- [37] V. B. Berestetskii and M. V. Terent'ev, Yad. Fiz. **24**, 1044 (1976) [Sov. J. Nucl. Phys. **24**, 547 (1976)]; **25**, 653 (1977) [**25**, 347 (1977)].
- [38] B. L. G. Bakker, L. A. Kondratyuk, and M. V. Terent'ev, Nucl. Phys. **B158**, 497 (1979).
- [39] I. G. Aznauryan, A. S. Bagdasaryan, and N. L. Ter-Isaakyan, Phys. Lett. **112B**, 393 (1982).
- [40] P. L. Chung, F. Coester, B. D. Keister, and W. N. Polyzou, Phys. Rev. C **37**, 2000 (1988); P. L. Chung and F. Coester, Phys. Rev. D **44**, 229 (1991); B. D. Keister and W. N. Polyzou, Adv. Nucl. Phys. **20**, 225 (1991).
- [41] F. Schlumpf and S. Brodsky, Phys. Lett. B **360**, 1 (1995).
- [42] F. Schlumpf, Phys. Rev. D **47**, 4114 D (1993); **48**, 4478 (1993); arXiv:hep-ph/9211255.
- [43] M. Hamermesh, *Group Theory and its Application to Physical Problems*, (Addison-Wesley, Reading, MA, 1964).
- [44] W. Xu *et al.*, Phys. Rev. Lett. **85**, 2900 (2000).
- [45] W. Xu *et al.*, (Jefferson Lab E95-001 Collaboration), Phys. Rev. C **67**, 012201 (2003).
- [46] M. Diehl, Nucl. Phys. B, Proc. Suppl. **161**, 49 (2006).
- [47] B. D. Milbrath *et al.* (Bates FPP Collaboration), Phys. Rev. Lett. **80**, 452 (1998); **82**, 2221(E) (1999).
- [48] M. K. Jones *et al.* (Jefferson Lab Hall A Collaboration), Phys. Rev. Lett. **84**, 1398 (2000).
- [49] V. Punjabi *et al.*, Phys. Rev. C **71**, 055202 (2005); **71**, 069902 (2005).
- [50] G. Ron *et al.* (JLab Hall A Collaboration), Phys. Rev. C **84**, 055204 (2011).
- [51] C. B. Crawford *et al.*, Phys. Rev. Lett. **98**, 052301 (2007).
- [52] M. K. Jones *et al.* (Resonance Spin Structure Collaboration), Phys. Rev. C **74**, 035201 (2006).
- [53] G. MacLachlan *et al.*, Nucl. Phys. **A764**, 261 (2006).
- [54] X. Jahn *et al.*, Phys. Lett. B **705**, 59 (2011).
- [55] A. J. R. Puckett *et al.*, Phys. Rev. Lett. **104**, 242301 (2010).
- [56] O. Gayou *et al.* (Jefferson Lab Hall A Collaboration), Phys. Rev. Lett. **88**, 092301 (2002).
- [57] R. C. Walker *et al.*, Phys. Rev. D **49**, 5671 (1994).
- [58] A. J. R. Puckett *et al.*, Phys. Rev. C **85**, 045203 (2012).
- [59] V. J. Lachniet *et al.* (CLAS Collaboration), Phys. Rev. Lett. **102**, 192001 (2009).
- [60] W. Bartel *et al.*, Nucl. Phys. **B58**, 429 (1973).
- [61] B. Anderson *et al.*, Phys. Rev. C **75**, 034003 (2007).
- [62] R. G. Arnold *et al.*, Phys. Rev. Lett. **61**, 806 (1988).
- [63] A. Lung *et al.*, Phys. Rev. Lett. **70**, 718 (1993).
- [64] G. Kubon *et al.*, Phys. Lett. B **524**, 26 (2002).
- [65] H. Anklin *et al.*, Phys. Lett. B **428**, 248 (1998).
- [66] G. G. Simon, C. Schmitt, F. Borkowski, and V. H. Walther, Nucl. Phys. **A333**, 381 (1980).
- [67] L. E. Price, J. R. Dunning, M. Goitein, K. Hanson, T. Kirk, and R. Wilson, Phys. Rev. D **4**, 45 (1971).
- [68] C. Berger, V. Burkert, G. Knop, B. Langenbeck, and K. Rith, Phys. Lett. **35B**, 87 (1971).
- [69] K. M. Hanson, J. R. Dunning, M. Goitein, T. Kirk, and L. E. Price, Phys. Rev. D **8**, 753 (1973).
- [70] S. Dieterich *et al.*, Phys. Lett. B **500**, 47 (2001).
- [71] C. Herberg *et al.*, Eur. Phys. J. A **5**, 131 (1999).
- [72] I. Passchier *et al.*, Phys. Rev. Lett. **82**, 4988 (1999).
- [73] T. Eden *et al.*, Phys. Rev. C **50**, R1749 (1994).
- [74] M. Ostrick *et al.*, Phys. Rev. Lett. **83**, 276 (1999).
- [75] J. Golak, G. Ziemer, H. Kamada, H. Witala, and W. Glockle, Phys. Rev. C **63**, 034006 (2001).
- [76] R. Madey *et al.* (Jefferson Lab E93-038 Collaboration), Phys. Rev. Lett. **91**, 122002 (2003).
- [77] H. Zhu *et al.* (Jefferson Lab E93-026 Collaboration), Phys. Rev. Lett. **87**, 081801 (2001).
- [78] D. Rohe *et al.*, Phys. Rev. Lett. **83**, 4257 (1999).
- [79] R. Schiavilla and I. Sick, Phys. Rev. C **64**, 041002 (2001).
- [80] I. V. Anikin, M. A. Ivanov, N. B. Kulimanova and V. E. Lyubovitskij, Z. Phys. C **65**, 681 (1995); M. A. Ivanov, M. P. Locher and V. E. Lyubovitskij, Few Body Syst. **21**, 131 (1996) M. A. Ivanov, V. E. Lyubovitskij, J. G. Körner and P. Kroll, Phys. Rev. D **56**, 348 (1997); A. Faessler, T. Gutsche, B. R. Holstein, M. A. Ivanov, J. G. Korner and V. E. Lyubovitskij, Phys. Rev. D **78**, 094005 (2008); A. Faessler, T. Gutsche, M. A. Ivanov, J. G. Korner and V. E. Lyubovitskij, Phys. Rev. D **80**, 034025 (2009); T. Branz, A. Faessler, T. Gutsche, M. A. Ivanov, J. G. Korner, V. E. Lyubovitskij and B. Oehl, Phys. Rev. D **81**, 114036 (2010).
- [81] L. Tiator and M. Vanderhaeghen, Phys. Lett. B **672**, 344 (2009).

### Appendix A: Coefficients $C_{S_{12}, S'_{12}}^{SS'}$

The coefficients  $C_{S_{12}, S'_{12}}^{SS'}$  defined in Sec.II A with Eq. (6) have the following explicit expression

$$C_{00}^{\frac{1}{2}\frac{1}{2}}(\boldsymbol{\lambda}_\perp, \boldsymbol{\Lambda}_\perp; \mu, \mu') = \frac{N_0}{D} \left( \delta_{\mu, \mu'} (m + (1-\eta)\mathcal{M}_0) - \delta_{\mu, -\mu'} (\Lambda_1(-1)^{\frac{1}{2}-\mu'} + i\Lambda_2) \right) \quad (\text{A1})$$

$$C_{00}^{\frac{1}{2}\frac{1}{2}*}(\boldsymbol{\lambda}_\perp, \boldsymbol{\Lambda}'_\perp; \bar{\mu}, \mu'') = \frac{N_0}{D} \left( \delta_{\bar{\mu}, \mu''} (m + (1-\eta)\mathcal{M}'_0) - \delta_{\bar{\mu}, -\mu''} (\Lambda'_1(-1)^{\frac{1}{2}-\mu''} - i\Lambda'_2) \right) \quad (\text{A2})$$

$$C_{10}^{\frac{1}{2}\frac{1}{2}}(\boldsymbol{\lambda}_\perp, \boldsymbol{\Lambda}_\perp; \mu, \mu') = -\frac{1}{D} \frac{1}{\sqrt{3}} \left\{ (m + (1-\eta)\mathcal{M}_0) \times \delta_{\mu, -\mu'} \left[ (2m + \eta\mathcal{M}_0)(\lambda_1(-1)^{\frac{1}{2}-\mu'} + i\lambda_2) - (1-2\xi)m(\Lambda_1(-1)^{\frac{1}{2}-\mu'} + i\Lambda_2) \right] + (2m + \eta\mathcal{M}_0)\delta_{\mu, \mu'} \left[ \boldsymbol{\lambda}_\perp \cdot \boldsymbol{\Lambda}_\perp + i[\boldsymbol{\lambda}_\perp \times \boldsymbol{\Lambda}_\perp]_3(-1)^{\frac{1}{2}-\mu'} \right] + \delta_{\mu, \mu'} (1-2\xi)m\boldsymbol{\Lambda}_\perp^2 \right\} \quad (\text{A3})$$

$$C_{10}^{\frac{3}{2}\frac{1}{2}}(\boldsymbol{\lambda}_\perp, \boldsymbol{\Lambda}_\perp; \mu, \mu') = \frac{1}{D} \frac{1}{\sqrt{2}} \left\{ \frac{1}{\sqrt{3}} \delta_{\mu, -\mu'} (m + (1-\eta)\mathcal{M}_0) \times \left[ (2m + \eta\mathcal{M}_0)(\lambda_1 + i\lambda_2(-1)^{\frac{1}{2}-\mu'}) - (1-2\xi)m(\Lambda_1 + i\Lambda_2(-1)^{\frac{1}{2}-\mu'}) \right] + (m + (1-\eta)\mathcal{M}_0) \left[ (2m + \eta\mathcal{M}_0)(\lambda_1\delta_+ + i\lambda_2\delta_-) - (1-2\xi)m(\Lambda_1\delta_+ + i\Lambda_2\delta_-) \right] - (2m + \eta\mathcal{M}_0) \times \left[ \frac{1}{\sqrt{3}} \delta_{\mu, \mu'} \left( \boldsymbol{\lambda}_\perp \cdot \boldsymbol{\Lambda}_\perp (-1)^{\frac{1}{2}-\mu'} + i[\boldsymbol{\lambda}_\perp \times \boldsymbol{\Lambda}_\perp]_3 \right) + (\lambda_1\Lambda_1 - \lambda_2\Lambda_2)\Delta_- + i(\lambda_1\Lambda_2 + \lambda_2\Lambda_1)\Delta_+ \right] + (1-2\xi)m \left[ \frac{1}{\sqrt{3}} \delta_{\mu, \mu'} (-1)^{\frac{1}{2}-\mu'} \boldsymbol{\Lambda}_\perp^2 + (\Lambda_1^2 - \Lambda_2^2)\Delta_- + 2i\Lambda_1\Lambda_2\Delta_+ \right] \right\} \quad (\text{A4})$$

$$C_{11}^{\frac{1}{2}\frac{1}{2}}(\boldsymbol{\lambda}_\perp, \boldsymbol{\Lambda}_\perp; \mu, \mu') = \frac{1}{D} \left\{ \delta_{\mu, \mu'} \left[ (m + (1-\eta)\mathcal{M}_0)(u - \frac{1}{3}\boldsymbol{W}_\perp \cdot \boldsymbol{V}_\perp) - \frac{2}{3}\boldsymbol{\Gamma}_\perp \cdot \boldsymbol{\Lambda}_\perp - \frac{i}{3}(m + (1-\eta)\mathcal{M}_0)\Gamma_2 \right] + \delta_{\mu, \mu'} (-1)^{\frac{1}{2}-\mu'} \left[ \frac{1}{3}(m + (1-\eta)\mathcal{M}_0)\Gamma_1 + \frac{2i}{3}\Gamma_2\Lambda_1 \right] + \delta_{\mu, -\mu'} \left[ \frac{2}{3}(m + (1-\eta)\mathcal{M}_0)\Gamma_2 + \frac{2i}{3}\Lambda_1[\boldsymbol{W}_\perp \times \boldsymbol{V}_\perp]_3 + i\left(\frac{1}{3}\Lambda_2(u - \boldsymbol{W}_\perp \cdot \boldsymbol{V}_\perp) - \frac{2}{3}\Lambda_2(W_1V_1 - W_2V_2)\right) \right] + \delta_{\mu, -\mu'} (-1)^{\frac{1}{2}-\mu'} \left[ \frac{2}{3}(m + (1-\eta)\mathcal{M}_0)\Gamma_1 + \frac{1}{3}\Lambda_1(u - \boldsymbol{W}_\perp \cdot \boldsymbol{V}_\perp) - \frac{2}{3}\Lambda_1(W_1V_1 - W_2V_2) - i\left(\frac{2}{3}\Lambda_2[\boldsymbol{W}_\perp \times \boldsymbol{V}_\perp]_3 + \frac{1}{3}[\boldsymbol{\Gamma}_\perp \times \boldsymbol{\Lambda}_\perp]_3 \right) \right] \right\} \quad (\text{A5})$$

$$C_{11}^{\frac{3}{2}\frac{1}{2}}(\boldsymbol{\lambda}_\perp, \boldsymbol{\Lambda}_\perp; \mu, \mu') = \frac{1}{D} \frac{1}{\sqrt{2}} \left\{ \times \delta_{\mu, \mu'} \left[ \frac{1}{3}(m + (1-\eta)\mathcal{M}_0)\Gamma_1 - i[\boldsymbol{\Gamma}_\perp \times \boldsymbol{\Lambda}_\perp]_3 \right] + \delta_{\mu, \mu'} (-1)^{\frac{1}{2}-\mu'} \left[ \frac{2}{3}(m + (1-\eta)\mathcal{M}_0)\boldsymbol{W}_\perp \cdot \boldsymbol{V}_\perp + (\Gamma_1\Lambda_1 + \frac{1}{3}\Gamma_2\Lambda_2) - i\frac{1}{3}(m + (1-\eta)\mathcal{M}_0)\Gamma_2 \right] + \delta_{\mu, -\mu'} \left[ \frac{1}{3}(m + (1-\eta)\mathcal{M}_0)\Gamma_1 + \frac{2}{3}\Lambda_1(u - \boldsymbol{W}_\perp \cdot \boldsymbol{V}_\perp) + \frac{2}{3}\Lambda_1(W_1V_1 - W_2V_2) + i\left(\frac{2}{3}\Lambda_2[\boldsymbol{W}_\perp \times \boldsymbol{V}_\perp]_3 + \frac{1}{3}(\Gamma_2\Lambda_1 + \Gamma_1\Lambda_2)\right) \right] + \delta_{\mu, -\mu'} (-1)^{\frac{1}{2}-\mu'} \left[ -\frac{2}{3}\Lambda_1[\boldsymbol{W}_\perp \times \boldsymbol{V}_\perp]_3 + \frac{1}{3}(\Gamma_1\Lambda_1 - \Gamma_2\Lambda_2) + i\left(\frac{1}{3}(m + (1-\eta)\mathcal{M}_0)\Gamma_2 + \frac{2}{3}\Lambda_2(u - \boldsymbol{W}_\perp \cdot \boldsymbol{V}_\perp) - \frac{2}{3}\Lambda_2(W_1V_1 - W_2V_2)\right) \right] + \frac{\Delta_-}{\sqrt{3}} \left[ -2(m + (1-\eta)\mathcal{M}_0)(W_1V_1 - W_2V_2) + \Gamma_1\Lambda_1 - \Gamma_2\Lambda_2 \right] + \frac{i\Delta_+}{\sqrt{3}} \left[ -2(m + (1-\eta)\mathcal{M}_0)[\boldsymbol{W}_\perp \times \boldsymbol{V}_\perp]_3 + \Gamma_2\Lambda_1 + \Gamma_1\Lambda_2 \right] + \frac{\delta_-}{\sqrt{3}} \left[ \boldsymbol{\Gamma}_\perp \cdot \boldsymbol{\Lambda}_\perp + i\Lambda_2u \right] + \frac{\delta_+}{\sqrt{3}} \left[ 2\Lambda_1u - i[\boldsymbol{\Gamma}_\perp \times \boldsymbol{\Lambda}_\perp]_3 \right] \right\} \quad (\text{A6})$$

where  $\boldsymbol{\lambda}_\perp$  and  $\boldsymbol{\Lambda}_\perp$  are defined in Eq. (7) and we use the following notations:

$$\mathbf{W}_\perp = \boldsymbol{\lambda}_\perp + \xi \boldsymbol{\Lambda}_\perp, \quad \mathbf{V}_\perp = \boldsymbol{\lambda}_\perp - (1 - \xi) \boldsymbol{\Lambda}_\perp, \quad (\text{A7})$$

$$\boldsymbol{\Gamma}_\perp = \eta(1 - \xi) \mathcal{M}_0 \boldsymbol{\lambda}_\perp + (m + (1 - \eta) \mathcal{M}_0) \boldsymbol{\Lambda}_\perp, \quad (\text{A8})$$

$$u = (m + \eta \xi \mathcal{M}_0)(m + \eta(1 - \xi) \mathcal{M}_0) \quad (\text{A9})$$

$$\Delta_\pm(\mu, \mu') = \delta_{\mu, -3/2} \delta_{\mu', 1/2} \pm \delta_{\mu, 3/2} \delta_{\mu', -1/2} \quad (\text{A10})$$

$$\delta_\pm(\mu, \mu') = \delta_{\mu, -3/2} \delta_{\mu', -1/2} \pm \delta_{\mu, 3/2} \delta_{\mu', 1/2} \quad (\text{A11})$$

$$N_0 = m(m + (1 - \eta) \mathcal{M}_0) + \xi(1 - \xi) \eta^2 \mathcal{M}_0^2 - (\boldsymbol{\lambda}_\perp + \xi \boldsymbol{\Lambda}_\perp) \cdot (\boldsymbol{\lambda}_\perp - (1 - \xi) \boldsymbol{\Lambda}_\perp), \quad (\text{A12})$$

$$N'_0 = m(m + (1 - \eta) \mathcal{M}'_0) + \xi(1 - \xi) \eta^2 \mathcal{M}'_0{}^2 - (\boldsymbol{\lambda}_\perp + \xi \boldsymbol{\Lambda}'_\perp) \cdot (\boldsymbol{\lambda}_\perp - (1 - \xi) \boldsymbol{\Lambda}'_\perp), \quad (\text{A13})$$

$$D = \prod_{i=1}^3 d_i, \quad d_i = \sqrt{(m_i + x_i \mathcal{M}_0)^2 + \mathbf{k}_{\perp i}^2}. \quad (\text{A14})$$

The matrix  $A_{\bar{\mu}, \mu}$  used in Sect. IID in Eq. (37) has a form

$$A_{\bar{\mu}, \mu} = \begin{cases} -\frac{1}{3} \delta_{\mu, -\bar{\mu}} (-1)^{1/2-\mu}, & \text{if } S = \frac{1}{2}, \\ \frac{2}{3} (\delta_{\mu, \frac{1}{2}} \delta_{\bar{\mu}, -\frac{1}{2}} - \delta_{\mu, -\frac{1}{2}} \delta_{\bar{\mu}, \frac{1}{2}}) \\ -\sqrt{\frac{1}{3}} (\delta_{\mu, -\frac{3}{2}} \delta_{\bar{\mu}, -\frac{1}{2}} - \delta_{\mu, -\frac{1}{2}} \delta_{\bar{\mu}, -\frac{3}{2}}) \\ +\sqrt{\frac{1}{3}} (\delta_{\mu, \frac{3}{2}} \delta_{\bar{\mu}, \frac{1}{2}} - \delta_{\mu, \frac{1}{2}} \delta_{\bar{\mu}, \frac{3}{2}}), & \text{if } S = \frac{3}{2}. \end{cases} \quad (\text{A15})$$

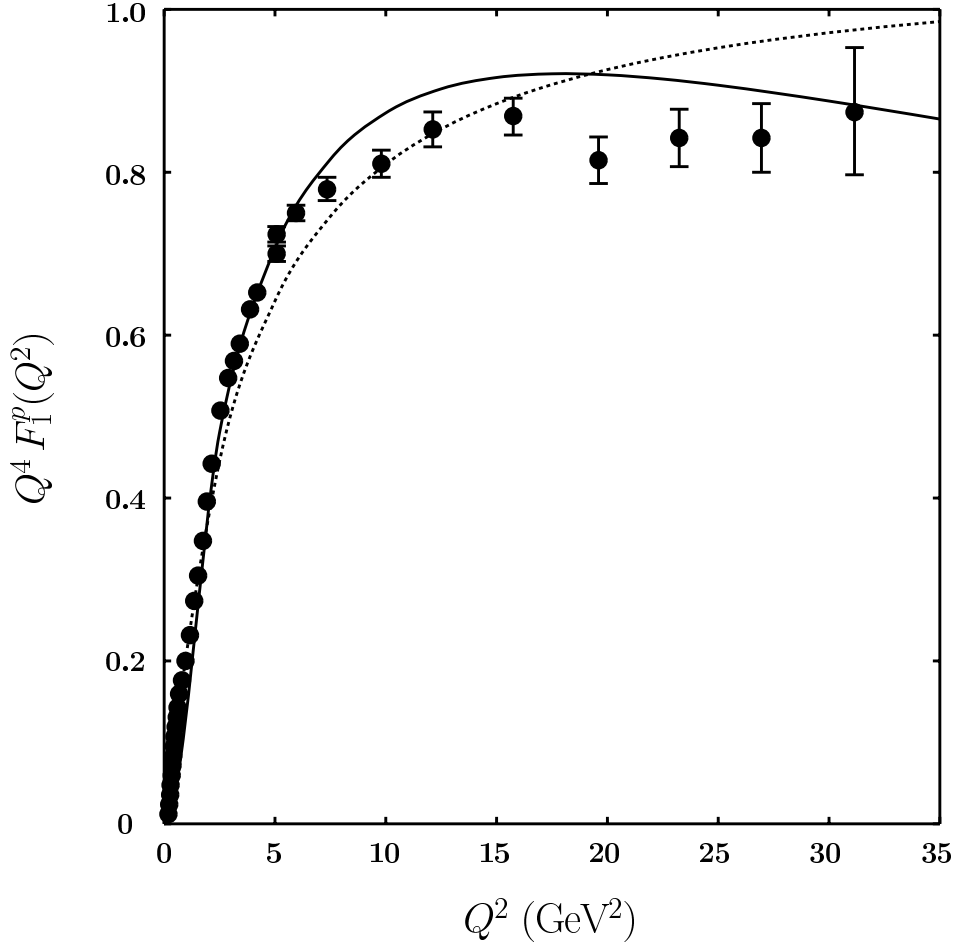


FIG. 1: Proton Dirac form factor multiplied with  $Q^4$ . Experimental data are taken from Ref. [46]. Prediction of the light-front quark model is given by the solid line, results from the AdS/QCD approach [33] are marked by the dotted line.

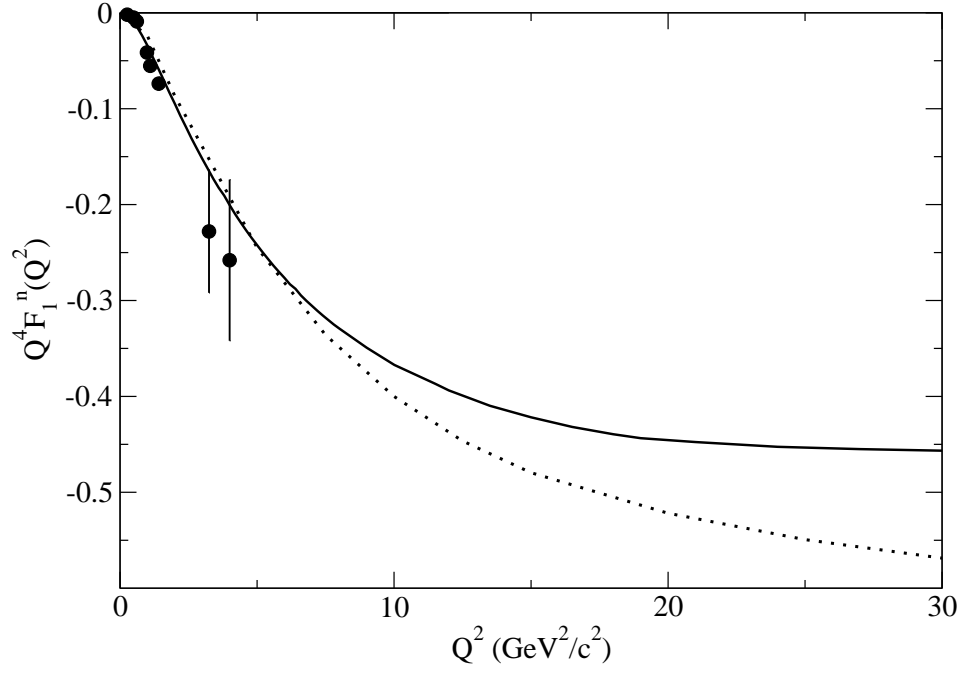


FIG. 2: Neutron Dirac form factor multiplied with  $Q^4$ . Experimental data are taken from Ref. [46]. Prediction of the light-front quark model is given by the solid line, results from the AdS/QCD approach [33] are marked by the dotted line.

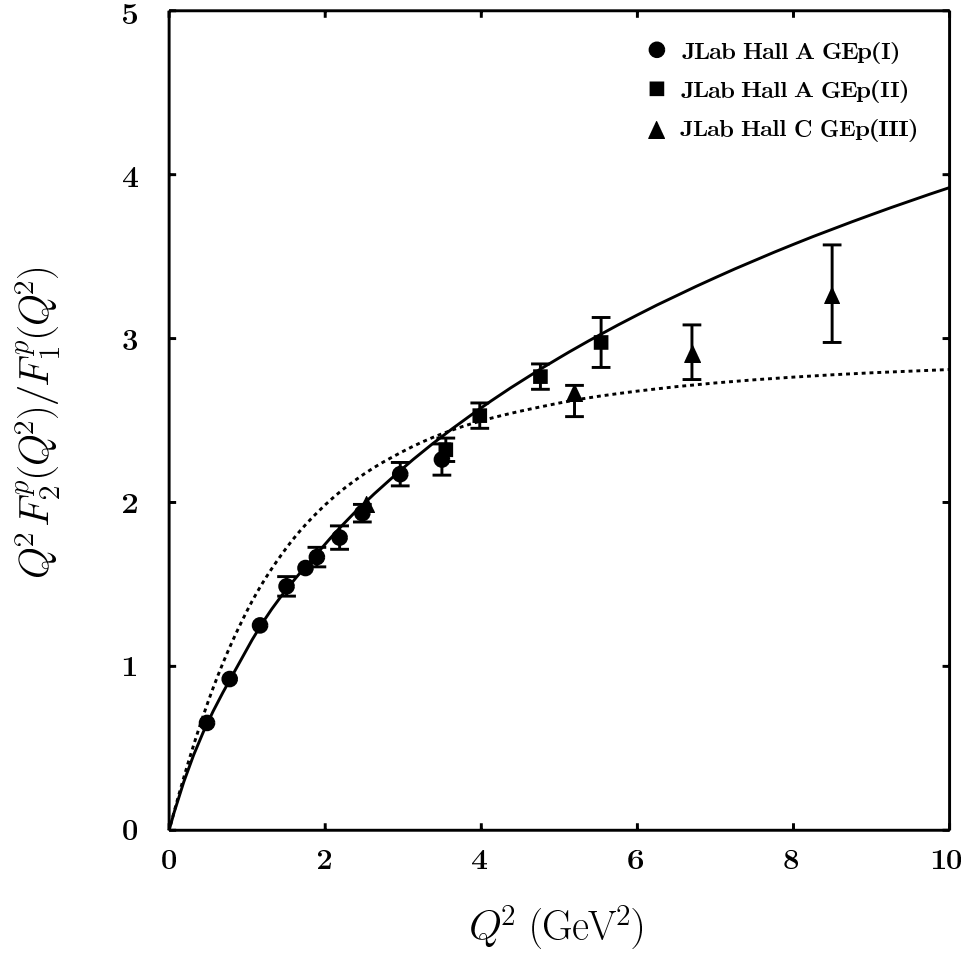


FIG. 3: Results for  $Q^2 F_2^p(Q^2)/F_1^p(Q^2)$ . Experimental data are taken from Refs. [47–55]. Prediction of the light-front quark model is given by the solid line, results from the AdS/QCD approach [33] are marked by the dotted line.

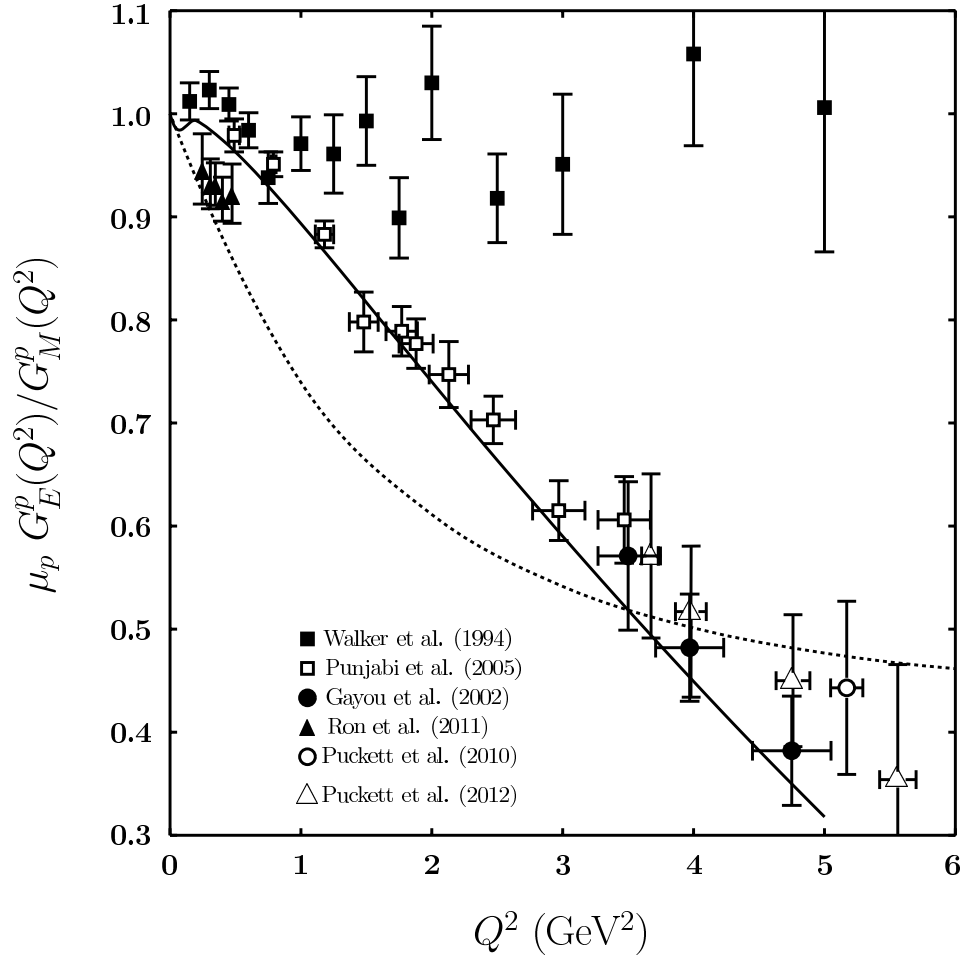


FIG. 4: Ratio  $\mu_p G_E^p(Q^2)/G_M^p(Q^2)$  in comparison to the experimental data taken from Refs. [49, 50, 56–58]. Prediction of the light-front quark model is given by the solid line, results from the AdS/QCD approach [33] are marked by the dotted line.

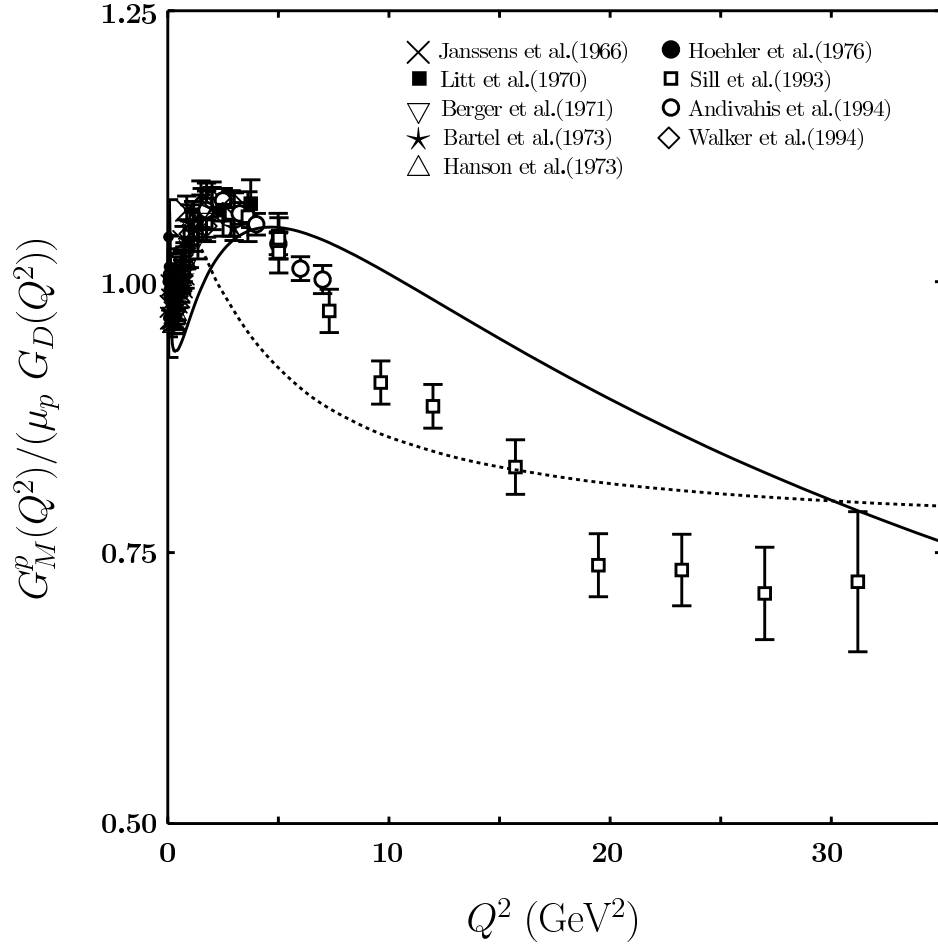


FIG. 5: Ratio  $G_M^p(Q^2)/(\mu_p G_D(Q^2))$ . Experimental data are taken from Refs. [49, 56, 57]. Prediction of the light-front quark model is given by the solid line, results from the AdS/QCD approach [33] are marked by the dotted line.

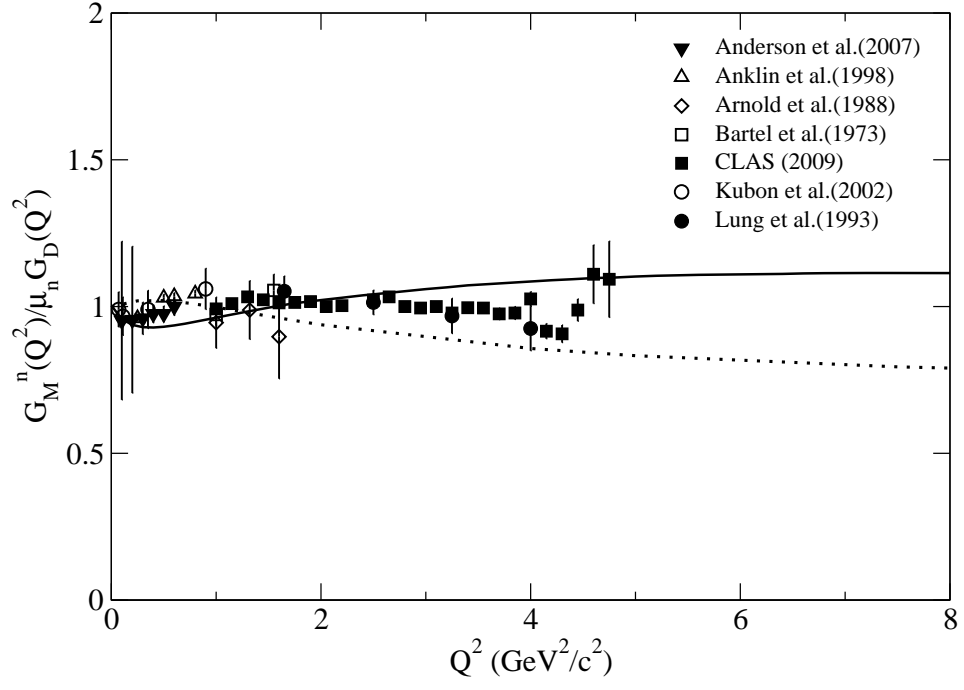


FIG. 6: Ratio  $G_M^n(Q^2)/(\mu_n G_D(Q^2))$ . Experimental data are taken from Refs. [59–65]. Prediction of the light-front quark model is given by the solid line, results from the AdS/QCD approach [33] are marked by the dotted line.

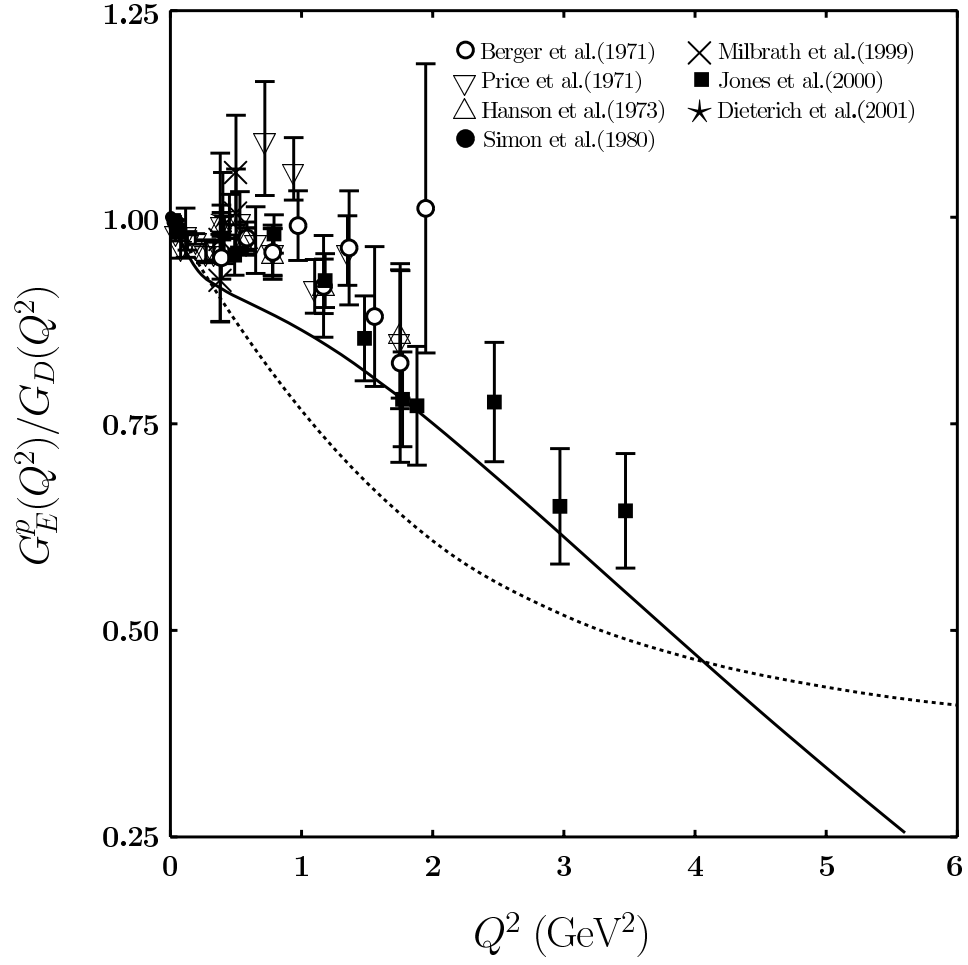


FIG. 7: Ratio  $G_E^p(Q^2)/G_D(Q^2)$ . Experimental data are taken from Refs. [47, 48, 56, 66–70]. Prediction of the light-front quark model is given by the solid line, results from the AdS/QCD approach [33] are marked by the dotted line.

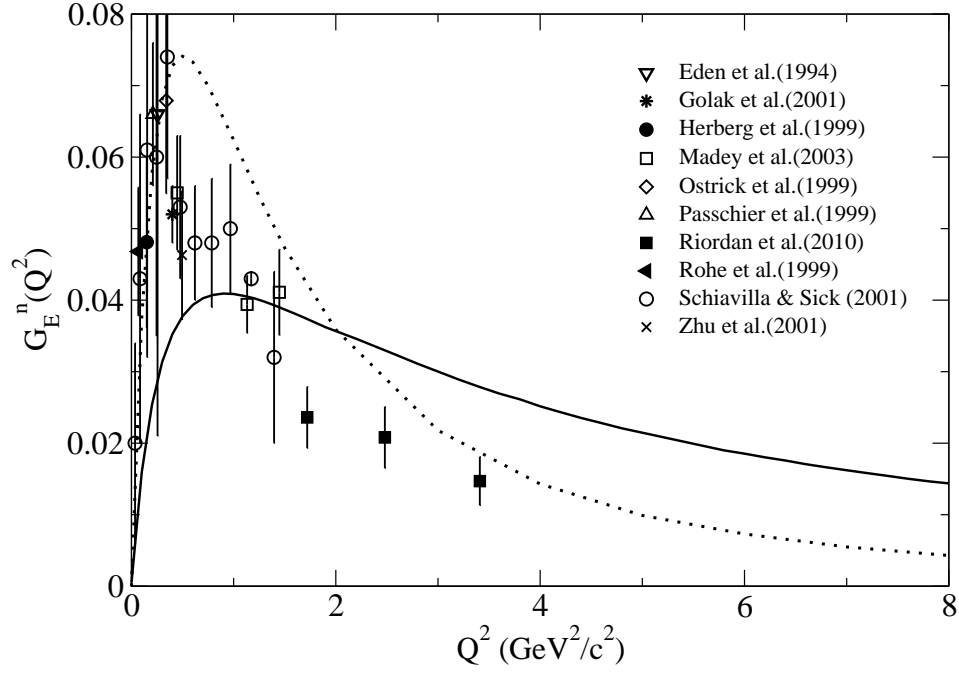


FIG. 8: The charge neutron form factor  $G_E^n(Q^2)$ . Experimental data are taken from Refs. [71–79]. Prediction of the light-front quark model is given by the solid line, results from the AdS/QCD approach [33] are marked by the dotted line.

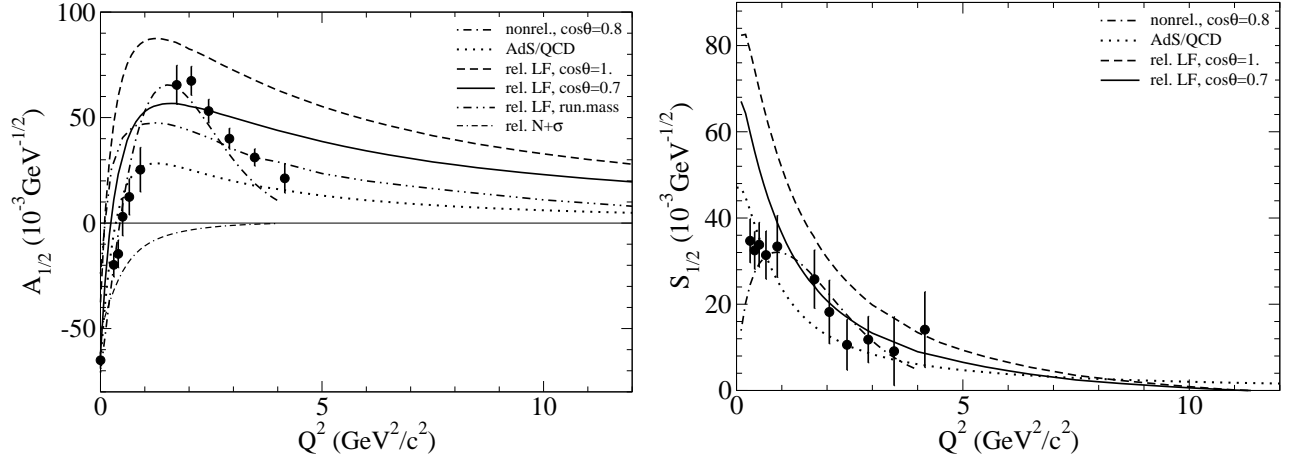


FIG. 9: The helicity amplitudes  $A_{1/2}$  and  $S_{1/2}$  (on the left and right pannels, respectively) for electroproduction of the Roper resonance on the proton. The data are from [1, 2]. The predictions of the light-front quark model are given by the short-dashed ( $\cos \theta = 1$ ), and the solid lines ( $\cos \theta = 0.7$ ); results from the AdS/QCD approach [33] are marked by the dotted line. Nonrelativistic results of Ref. [35] (the dashed dotted line) and the result of Ref. [28] for LF model with running quark masses (the double-dotted dashed line) are also shown for comparison. The  $A_{1/2}$  amplitude for hadronic  $N + \sigma$  molecular state are marked by the double-dashed dotted line (adopted from ref. [35]).